Journal of Structural Geology 33 (2011) 928–950

Contents lists available at ScienceDirect

Journal of Structural Geology

journal homepage: www.elsevier.com/locate/jsg

Structural development of a high-pressure collisional accretionary wedge: The Samaná complex, Northern Hispaniola

Javier Escuder-Viruete [a,*], Andrés Pérez-Estaún [b], Janet Gabites [c], Ángela Suárez-Rodríguez [d]

[a] Instituto Geológico y Minero de España, C. La Calera 1, 28760 Tres Cantos, Madrid, Spain
[b] Instituto Ciencias Tierra Jaume Almera-CSIC, Lluís Solé Sabarís s/n, 08028 Barcelona, Spain
[c] Pacific Centre for Isotopic and Geochemical Research, University of British Columbia, 6339 Stores Road, Vancouver, BC V6T-1Z4, Canada
[d] Instituto Geológico y Minero de España, Av. Real 1, 24006 León, Spain

ARTICLE INFO

Article history:
Received 25 August 2010
Received in revised form
16 February 2011
Accepted 21 February 2011
Available online 2 March 2011

Keywords:
Accretionary wedge
Ductile thrusting
High-pressure metamorphism
$^{40}Ar/^{39}Ar$ geochronology
Caribbean plate

ABSTRACT

The Samaná metamorphic complex exposes a segment of a high-pressure collisional accretionary wedge, built during Caribbean island arc-North America continental margin convergence. Combined detailed mapping, structural and metamorphic analysis, and $^{40}Ar/^{39}Ar$ geochronology show that the deformation can be divided into five main events. Early subduction-related D1 deformation and high-P/low-T M1 metamorphism under lawsonite blueschist (325–425 °C/12–18 kbar; Rincon Marbles and Santa Bárbara Schists lower structural nappes) and eclogite facies conditions (425–450 °C/18–20 kbar; Punta Balandra upper structural nappe), was followed by M2 decompression and cooling in the blueschist facies conditions during D2 folding, thrusting and nappe stacking. $^{40}Ar/^{39}Ar$ plateau ages and T-t/P-t estimations revealed Late Eocene to earliest Miocene retrograde M2 metamorphism in the different nappes for a consistent D2 top-to-the-ENE tectonic transport, which suggests a general northeastward progradation of deformation. The D3 event substantially modified the nappe stack and produced open to tight folds with amplitudes up to kilometer-scale and the D4 ductile to brittle normal shear zones and faults, and related subhorizontal folding, record a late extensional deformation, which also affects the whole nappe pile. Non-penetrative D3 and D4 fabrics indicate M3 cooling in and under the M3 greenschist-facies conditions. From the Miocene to the Present, the nappe pile was cut and laterally displaced by a D5 sinistral strike-slip and reverse fault system associated with the Septentrional fault zone.

1. Introduction

Accretionary wedges (or prisms) comprise materials that have been transferred from the lower plate to the upper plate in intra-oceanic or continental subduction zones. At all but the shallowest levels of the forearc, near the front of the wedge, these materials have been underthrust with the lower plate and accreted to the upper plate. This accretion process involves a downward migration of the subduction thrust. Thus, accretionary prisms constructed by this "underplating" process include faults that were for a period of time subduction thrusts. Depending on their depth of accretion, the rocks preserve a record of deformation and metamorphism during the burial in the lower plate, the accretion process at maximum depth, and exhumation in the upper plate. In addition to the faults active during the initial emplacement of their rocks, accretionary prisms can be cut by later reverse faults, or out-of-sequence thrusts, high-angle and detachment normal faults, and strike-slip fault systems (Ring and Brandon, 1994; Ring et al., 1999; Ring and Layer, 2003; Mann, 2007), which alter substantially their original architecture.

Progressive addition or underplating of material at the base of accretionary wedges may result in their uplift and exhumation. These exhumed rocks form usually nappes thrust towards the paleo-trech, of hectometric to kilometric thickness, with lower metamorphic units structurally overlain by higher metamorphic units (Kimura et al., 1996; Agard et al., 2001, 2009; Lister and Forster, 1996; Stanek et al., 2006). These nappes started to develop under high-pressure (P)/low-temperature (T) conditions, generally under blueschist facies conditions, suggesting that the early exhumation is accommodated by thrusting.

* Corresponding author. Tel.: +34 917287242.
E-mail addresses: j.escuder@igme.es (J. Escuder-Viruete), andres@ija.csic.es (A. Pérez-Estaún), jgabites@eos.ubc.ca (J. Gabites), a.suarez@igme.es (Á. Suárez-Rodríguez).

0191-8141/$ – see front matter © 2011 Elsevier Ltd. All rights reserved.
doi:10.1016/j.jsg.2011.02.006

However, recent petrological and geophysical data indicate that during intra-oceanic subduction the oceanic crust and the overlying sediments, part of which can be accreted to form the accretionary wedge, are also dragged at depth along the subduction plane into the so-called subduction channel (Cloos and Shreve, 1988). Therefore, exhumation of subducted rocks metamorphosed under high-P/low-T conditions may then take place in the wedge and/or in the channel (Platt, 1993; Ring et al., 1999; Jolivet et al., 2003; Agard et al., 2009; Guillot et al., 2009). Underthrusting, detachment faulting and erosion, which are the driving exhumation mechanisms for the sediments in the upper levels of the subduction channel, often preserve the continuity of the P–T conditions within the accreted sedimentary material (Agard et al., 2001; Yamato et al., 2007). In contrast, blueschist and eclogite mafic bodies are systematically associated with serpentinites and/or a mechanically weak matrix, and eclogites wrapped by a serpentinitic-matrix mélange mostly crop out in an internal position in the orogen (Wakabayashi, 1990; Guillot et al., 2004; Tsujimori et al., 2006). The exhumation of mafic oceanic rocks from the lower levels of the subduction channel was facilitated by their association with serpentinites, which would counterbalance their negative buoyancy and enhance mechanical decoupling (Hermann et al., 2000; Guillot et al., 2001; García-Casco et al., 2006; Agard et al., 2009). Finally, when a large continental piece (i.e., a passive margin or an isolated block) enters the subduction zone it may also be dragged by 'continental subduction', but generally only during a restricted period of time (c. 10 Ma; Ernst, 2005; Chopin, 2003), after which collision develops. The introduction of the low-density continental material is generally thought to be responsible for the choking of subduction, which then stops or jumps outboard of the continental block (e.g. Stern, 2004).

In this tectonic context, the igneous and metamorphic inliers outcropping in the Septentrional Cordillera and Samaná Peninsula of the northern Dominican Republic include part of an accretionary wedge, built during Mesozoic to Cenozoic convergence and collision between the Caribbean island-arc and the North America southern continental margin. In the part of the collisional acretionary wedge outcropping as a nappe pile on Samaná Peninsula, the aim of this work is: (1) to analyze the structural evolution of each nappe and its relationship to the metamorphic P–T paths; (2) to evaluate the obtained $^{40}Ar/^{39}Ar$ age data in the context of the tectonometamorphic history of the complex; and (3) to discuss possible exhumation mechanisms and structural settings for the high-P rocks, particularly for the mafic eclogite blocks, and its bearing within the framework of the northern Caribbean tectonics.

2. Regional setting

Located on the northern margin of the Caribbean plate, the tectonic collage of Hispaniola results from the oblique convergence of the Caribbean island-arc system with the North American plate, which began in the Cretaceous. The arc-related rocks are regionally overlain by Paleocene/Lower Eocene to Holocene siliciclastic and carbonate sedimentary rocks that post-date volcanic activity, and record the oblique arc-continent collision in the north, as well as the active subduction along the southern Hispaniola margin (Mann, 1999). Today, the oblique convergence between Caribbean and North America in Hispaniola is partitioned between plate boundary parallel motion on the Septentrional and Enriquillo strike-slip faults in the overriding plate, and plate boundary normal motion at the plate interface on the offshore low-angle subduction thrusts of the Northern Hispaniola fault and Los Muertos trench (Fig. 1; Mann et al., 2002; Manaker et al., 2008).

In the northern Dominican Republic, the Septentrional Cordillera-Samaná Peninsula geological domain is a composite of arc and oceanic derived units which were built during arc-continent convergence an accretionary wedge (Draper and Lewis, 1991). Accreted units outcrop in several inliers, termed El Cacheal, Palma Picada, Pedro Gracía, Puerto Plata, Río San Juan and Samaná complexes, which constitute the pre-Eocene igneous and metamorphic basement complexes of the Septentrional Cordillera (Fig. 1). These six complexes include metasedimentary rocks of the subducted continental margin of North America, serpentinitic-matrix mélanges containing blocks of blueschists and eclogites, ophiolitic fragments of the proto-Caribbean lithosphere, plutonic and volcanic rocks related with the Cretaceous Caribbean island-arc, and non-metamorphic rocks deposited in pre-collisional forearc sedimentary basins (Escuder-Viruete, 2008b). In Puerto Plata and Río San Juan complexes, the first foreland deposits associated to the collisional processes are the Paleocene?/Lower Eocene olistostromes of the lower Imbert Fm (Draper et al., 1994), which contain clastic elements derived from the Cretaceous volcanic arc, the metamorphosed ophiolites and, in minor amounts, the high-P metasediments derived from the subducted continental margin.

The Samaná complex (Fig. 2) consists of syntectonically metamorphosed pelitic, carbonate and mafic rocks, alternating in variable relative amounts. Joyce (1991) recognized a sequence of three metamorphic mineral zones, ranging from lawsonite-bearing schists in the NE to eclogites and garnet-blueschists presents as lenses in the SW. Rocks preserving relict primary structures and recrystallized to lawsonite+albite-bearing assemblages characterize Zone I (Santa Barbara unit; De Zoeten et al., 1991). A 1–2 km width narrow intermediate Zone II is defined by lawsonite + albite + glaucophane assemblages in mafic rocks. In the southern side of the peninsula, garnet + omphacite + phengite and garnet + clinozoisite+ glaucophane-bearing assemblages in intercalated mafic lenses and blocks within micaschists and marbles, define a Zone III (Punta Balandra unit). The metamorphic sequence represents a metamorphic profile generated during SW-dipping Cretaceous-Eocene subduction (Joyce, 1991). However, the increase in grade occurs over a short distance and it can be better explained by tectonic juxtaposition of units that were metamorphosed at different depths (Escuder-Viruete and Pérez-Estaún, 2006). Minimum P–T conditions achieved were about 13 ± 2 kbar and 450 ± 70 °C in the Punta Balandra unit and 7.5 ± 2 kbar and 320 ± 80 °C in the Santa Bárbara unit (Joyce, 1991; Gonçalves et al., 2000). Structural data and the pressure gap between them permitted Gonçalves et al. (2000) to deduce that the Punta Balandra unit is thrust over the Santa Bárbara unit and to interpret the metamorphic nappe stack of Samaná complex as a fragment of an accretionary wedge thrust onto the North American continental shelf.

The mafic eclogites, blueschists and other high-P rocks of the Punta Balandra unit are usually found as boulders in the rivers that drain the unit and flow to the beach of the Samaná Bay. They have been object of numerous petrological and geochemical studies (Perfit et al., 1982; Giaramita and Sorensen, 1994; Sorensen et al., 1997; Catlos and Sorensen, 2003; Zack et al., 2004; Escuder-Viruete and Pérez-Estaún, 2006), but without a precise indication of its structural context. Trace and major element geochemistry and Nd-isotopic patterns of eclogites and blueschists indicate that the protoliths originated at a mid-ocean ridge and a volcanic arc setting, and subsequently were metamorphosed and metasomatized in a mantle wedge above a subduction zone (Perfit et al., 1982; Joyce, 1991; Sorensen et al., 1997).

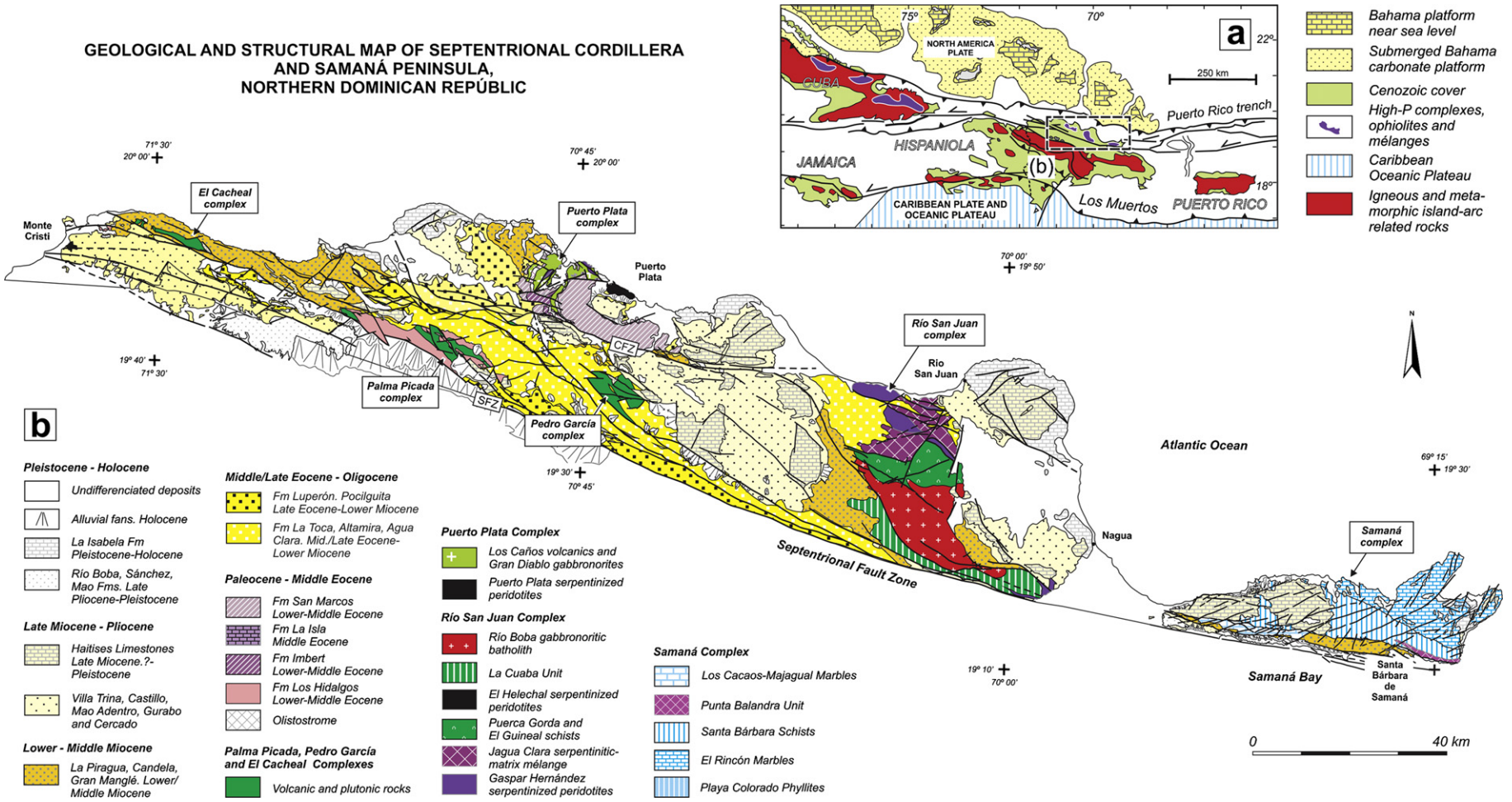

Fig. 1. (a) Map of the northeastern Caribbean plate margin. Box shows location of the northern Hispaniola area. (b) Geological map of Septentrional Cordillera and Samaná Peninsula greatly modified from Draper and Lewis (1991), Draper and Nagle (1991), Escuder-Viruete (2008a), and Escuder-Viruete (2009a). SFZ, Septentrional fault zone.

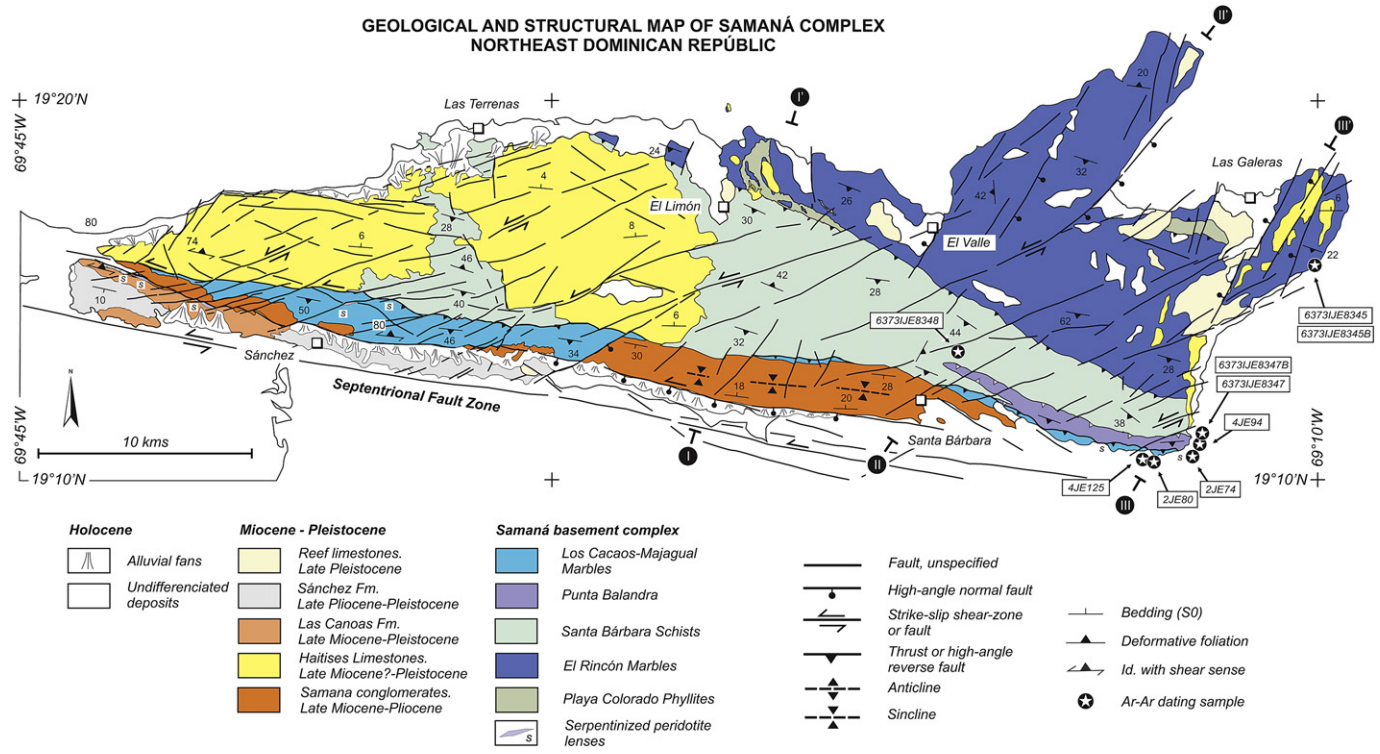

Fig. 2. Simplified geological and tectonic map of Samaná Peninsula modified from Joyce (1991) and Escuder-Viruete (2008a), showing major rock units, thrusts and faults (with barbs and ticks on the hanging wall sides), as well as representative structural attitudes of rocks. The different nappes are described in Table 1. The D2 Punta Balandra basal thrust put the nappe on top of the Santa Bárbara Schists nappe. The Majagual-Los cacaos basal thrust is a late-D2 structure reworked as a D4 mid- to low-angle extensional fault. Numerous strike-slip and normal D5 faults overprinted all earlier ductile contacts. Samaná Conglomerate fills a Neogene pull-apart basin. The Septentrional fault zone occurs onshore just south of the complex. Positions of cross-sections I–I', II–II' and III–III' (Fig. 3), serpentinized peridotite lenses (s) and locations of samples for Ar–Ar geochronology (stars) are indicated.

3. Geology of Samaná Peninsula

3.1. The metamorphic complex

Our mapping at the 1:50000 scale covered the whole Samaná Peninsula and complemented the work of Joyce (1991). The general geology of the Samaná Peninsula is composed of three elements (Escuder-Viruete, 2008a, b; Fig. 2): (1) a subduction-related metamorphic complex whose internal structure consists of a imbricate stack of discrete high-P nappes; (2) a group of Miocene coarse-grained siliciclastic rocks that are both in fault contact and unconformably overlie the metamorphic complex along the south coast; and (3) an unconformable cover of sub-horizontal Late Miocene to Pleistocene limestone formations. This study is only concerned with the metamorphic complex. The whole of the Samaná Peninsula is deformed by sinistral strike-slip and reverse faults associated with the (at least) earliest Miocene to Present movement of the Septentrional fault zone. This large-scale, subvertical fault zone occurs onshore just south of the complex.

The nappe stacking of the Samaná complex is essentially composed of high-P metasedimentary rocks. In ascending order the major tectonic nappes are: Playa Colorado Phyllite, Rincón Marbles, Santa Bárbara Schists, Punta Balandra, and Majagual-Los Cacaos Marbles. This nappe pile is described in Table 1. Cross-sections and orientation data (Figs. 3 and 4) show that the nappe pile dips to the S-SSW. Several additional points to have in account are described below.

The Playa Colorado Phyllite outcrops in a tectonic window at the NE sector of the complex. The Rincón Marbles consists of three lithologically distinct metacarbonate sub-units and, in the uppermost structural levels, also by Playa Colorado Phyllite-like metasediments, which suggests large-scale folding. In the Santa Bárbara Schists, the abundance and thickness of marble intercalations increases downwards. The Punta Balandra nappe is mainly composed of relatively coherent metasedimentary sequences metamorphosed to the lawsonite-eclogite and upper blueschist facies conditions. Mafic eclogites and garnet-bearing blueschists in the Punta Balandra nappe occur as spatially restricted lenses, boudins, layers or knockers within metasedimentary and/or Mg-rich mafic lithologies that display similar or slightly lower P–T mineral assemblages (Escuder-Viruete and Pérez-Estaún, 2006). Block sizes range from few centimeters to about 25 m. The unit also includes in the uppermost structural levels a <35 m-thick mélange-like sub-unit composed of meta-ophiolitic mafic to ultramafic blocks in a strongly sheared and retrograded serpentinitic and metapelitic matrix (Fig. 4). Mg-rich rinds enveloping blocks are here common. Serpentinized peridotites and serpentinite lenses also occur in the northern boundary of the Septentrional fault zone, which were tectonically interleaved with Tertiary rocks during Miocene to Present deformation.

3.2. Metamorphic history

Within the Samaná complex, the spatial distribution of the maximum P–T metamorphic conditions (Table 2, Fig. 5) reveal upper greenschist transitional to lower blueschist facies in the Playa Colorado Phyllites, blueschist and upper greenschist-facies in the El Rincón Marbles, upper blueschist (uppermost structural levels) and blueschist facies in the Santa Bárbara Schists, upper blueschist and eclogite facies in the Punta Balandra, and upper

Table 1
Geology of the nappes or structural units of Samaná Peninsula.

Nappes	Regional tectonic unit	Metamorphism (a)	General lithology	Comments
Majagual-Los Cacaos Marbles (uppermost nappe)	Accretionary prism. Subducted sediments of the continental margin	Upper to lower greenschist facies	Calcitic and dolomitic marbles, subordinate calcschists and phyllites	*Globotruncana* fossils yield Campanian-Maastrichtian age (b)
Punta Balandra (uppermost structural levels)	Accretionary prism. Ophiolitic material. Chaotic ductile to brittle disruption; mélange-like internal structure	Eclogite facies followed by retrograde blueschist facies	Metabasic blocks wrapped in serpentinitic schists or in a metapelitic mechanically weak matrix mélange (<35 m thick). Serpentinized peridotite lenses	Mafic protholiths of IAT, MORB and BABB affinity. Subducted either oceanic crust (and mantle) and arc mafic material. Resembles eclogite association of Río San Juan complex
Punta Balandra	Accretionary prism. Subducted sediments of the continental margin	Upper blueschist and eclogite facies	Marbles, calcschists and micaschists, with minor mafic lenses of eclogites and Grtblueschists	Coherent internal ductile structure. Mafic protholiths of MORB and BABB affinity
Santa Bárbara Schists	Accretionary prism. Subducted sediments of the distal continental margin	Blueschist and upper blueschist facies (uppermost structural levels)	Micaschists and calcschists, with marbles and quartzschists intercalations	Abundant marble intercalations at the botton
El Rincón Marbles (three lithological subunits)	Accretionary prism. Subducted carbonate platform of the proximal continental margin	Blueschist and upper greenschist facies	Banded clear marbles, calcschists and phyllites (upper), fine-grained dark marbles (middle) and massive white marbles (lower)	>3000 m thick sequence of texturally heterogeneous calcitic marbles
Playa Colorado Phyllites (lowermost nappe)	Accretionary prism. Subducted sediments of the distal continental margin	Lower greenschist transitional to upper greenschist facies	Phyllites, chlorite-schists, calcschists and chert	Similar lithologic association occurs at top El Rincón Marbles

(a) Refered to peak P–T conditions of Cretaceous and Tertiary metamorphism; (b) Weaver et al. (1976).

greenschist and blueschist facies in the Majagual-Los Cacaos Marbles (Fig. 6). Therefore, the peak pressure conditions increase structurally upward. A pronounced metamorphic break (up to 10 kbar) occurs towards lower pressures and temperatures in the marbles above the Punta Balandra nappe.

The general evolution in P–T conditions of the complex is characterized by three metamorphic events (M1 to M3; Escuder-Viruete et al., 2011). As will be shown below, maximum high-P assemblages in the Samaná complex developed during the first deformational event (D1) and are therefore referred to as M1. The associated chlorite-phengite±paragonite S1 foliation in metapelites and calcschists was porphyroblastically overgrown by lawsonite, rare chloritoid, glaucophane, and garnet during a syn- to late-D1 growth event (Fig. 7). Other occurrences or relics of the high-P mineral assemblage Fe–Mg carpholite + chlorite + phengite + quartz±chloritoid are found within quartz- and calcite-bearing veins or segregations in the Santa Bárbara Schists (Fig. 7h). Fibrous mesoscopic appearance and characteristic light green silvery colour of such metamorphic veins resemble the typical Fe–Mg carpholite pseudomorphs described in the literature (Goffé and Bousquet, 1997; Agard et al., 2001; Rimmelé et al., 2005). During the D2 deformation, the M1 high-P assemblages in the Samaná complex were replaced by M2 blueschist and transitional upper greenschist-facies assemblages (Fig. 5). Most of metasediments show retrogressed M2 mineral assemblages composed by phengite + chlorite + paragonite + quartz+calcite/dolomite. The retrograde P–T path is constrained by the decay of Fe–Mg carpholite to chlorite and phengite forming pseudomorphs, which indicates decompression under isothermal or cooling conditions after the M1 high-P stage. Maximum temperature in the uppermost structural levels of the Santa Bárbara Schists nappe occurred during the D2 deformation and therefore the upper blueschists-facies event is regarded here as M2. In calcschists and metapelites, it was characterized by the prograde formation of epidote, glaucophane, winchite and biotite. A subsequent greenschist-facies metamorphic event (M3) was mainly recorded by the retrograde formation of actinolite, chlorite, epidote and white mica in metabasites of the Punta Balandra nappe. In these rocks, Escuder-Viruete and Pérez-Estaún (2006) estimated about 5–8 kbar and 300–400 °C for M3, which occurred during further decompression and cooling (Table 2).

3.3. Age data

The age of the sedimentary protoliths of the Samaná complex is ill defined due to intense deformation and rarity of fossils. A Jurassic to Campanian-Maastrichtian age is inferred, based on lithological regional criteria (Joyce, 1991) and the fossil record of *Globotruncana* (Weaver et al., 1976) and *Belemnites* (Iturralde-Vinent et al., 2006, com. pers.).

The age of the tectonometamorphic events has been established only for the eclogite blocks enclosed in the Punta Balandra nappe. Imprecise but remarkably similar Sm-Nd isochron ages of 78 ± 30 Ma (Perfit et al., 1982), 84 ± 22 Ma (Joyce, 1991) and 86 ± 47 Ma (Grt-Omp-whole rock; Escuder-Viruete and Pérez-Estaún, 2004) suggest that the M1 eclogitic event formed during the final stages of subduction of the mafic protoliths during the Late Cretaceous to Early Eocene. Cooling of the eclogite blocks bellow ~350–400 °C (assumed phengite closure temperature) took place between Eocene and Late Oligocene, according the phengite K–Ar ages of 38 ± 2 Ma obtained by Joyce and Aronson (1987), and the phengite $^{40}Ar/^{39}Ar$ ages between 48.9 ± 3.7 and 25.5 ± 2.5 Ma (n = 48; average 37.8 ± 2.6 Ma, MSWD = 13) obtained by Catlos and Sorensen (2003). Consistently, Gonçalves et al. (2000) obtains an Rb–Sr isochron age of 32 ± 2 Ma (whole rock-phengite) in the eclogites. Late Eocene to Early Oligocene $^{40}Ar/^{39}Ar$ plateau cooling ages are also obtained from phengite in banded eclogite (35.65 ± 0.73 Ma) and foliated garnet glaucophanite (33.68 ± 0.47 Ma) by Escuder-Viruete and Pérez-Estaún (2004), which are attributed to the regional exhumation of the Punta Balandra nappe triggered by the oblique collision of the Bahamas Platform beneath the Caribbean island arc.

4. Deformation history

Detailed structural studies were conducted at the tectonic contacts and within the different tectonometamorphic nappes of

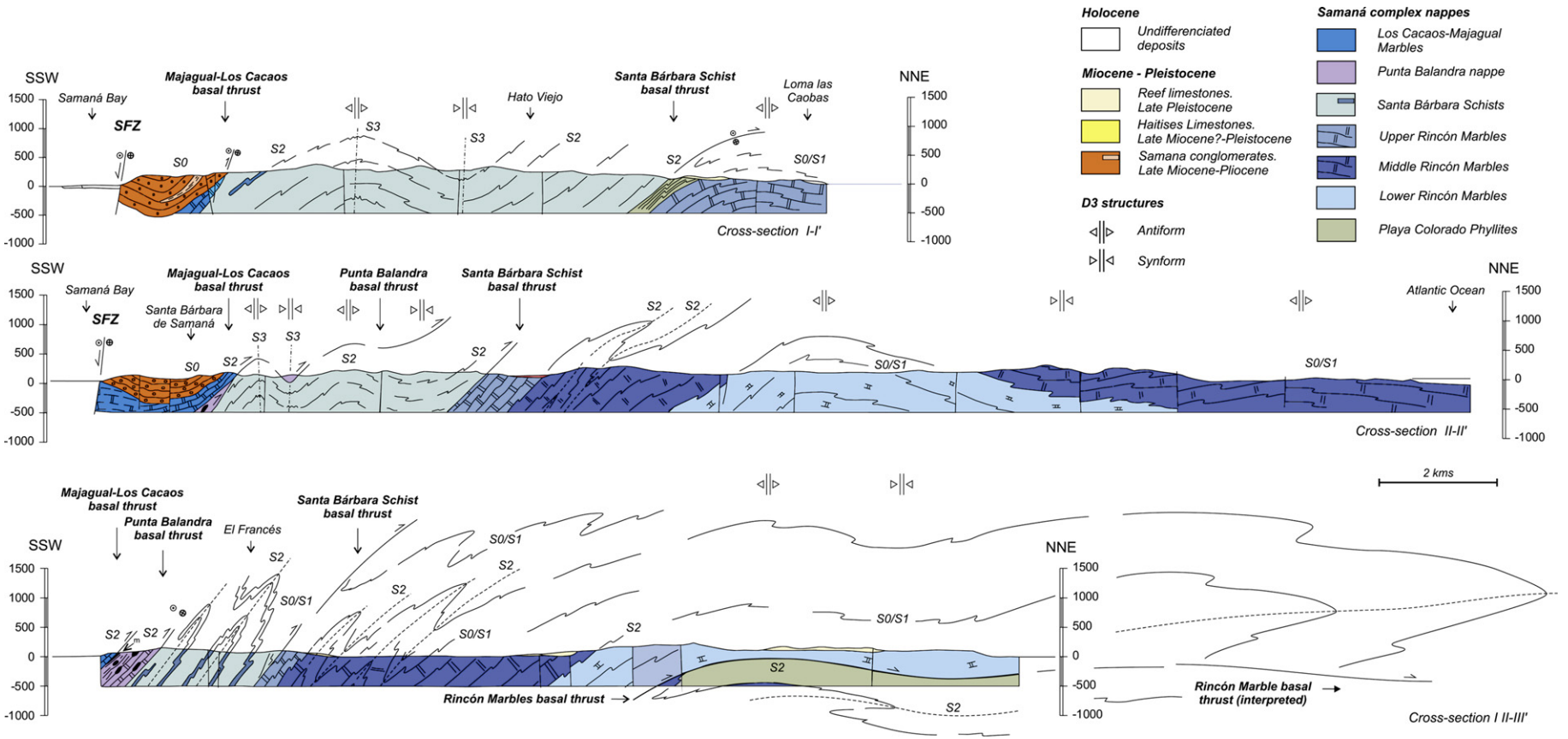

Fig. 3. Serial cross-sections through Samaná Peninsula showing its general architecture (refer to Fig. 2 for transect positions). The trace of main foliation illustrates the general SE-dipping structure (see also Fig. 4), which is re-folded by open D3 folds with amplitudes up to kilometer-scale. The large-scale D2 fold structured in the Rincón Marbles nappe is interpreted from the projection in the cross-section III—III' plane of: the internal structure of the nappe in three marble sub-units, the tectonic window of Playa Colorada nappe and the D2-synform of Playa Colorada-like phyllites outcropping near El Limón locality (Fig. 2).

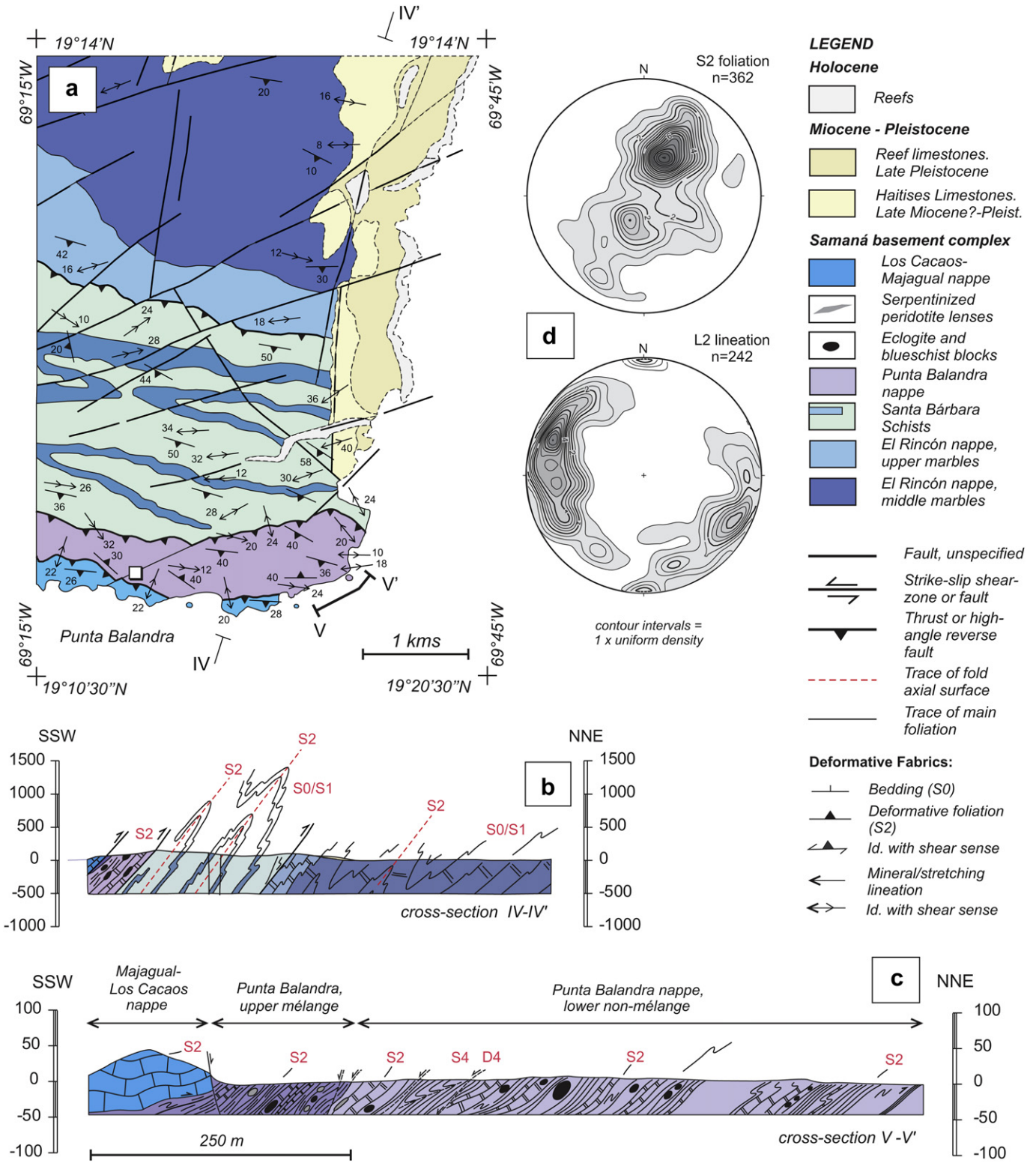

Fig. 4. Detailed map (a) and cross-sections through southeastern Samaná complex showing large-scale tight D2 folding of the marbles in the Santa Bárbara Schists nappe (b), and the structural relations between upper mélange and lower non-mélange parts of Punta Balandra nappe underlying the Majagual-Los Cacaos Marble nappe. (d) Stereographic projections of D2 fabric elements in the metamorphic complex.

the Samaná complex. Based mainly on overprinting criteria in macro and mesostructures and microstructural relations of mineral parageneses, we recognized sets of structures formed during five major deformational events (D1-D5). In general, D2 is the dominant ductile deformation in the complex; earlier structures and fabrics have been substantially modified and transposed and therefore only a little information about the geometry and kinematics of D1 exists. D3 to D5 deformations are discontinuous and much less penetrative, recording the evolution from ductile to brittle conditions of deformation.

Table 2
Metamorphic data of the nappes or structural units of Samaná Peninsula.

Nappe or structural unit	Metamorphic event	Lithology and mineral assemblages (a)	P–T conditions of deformational events
Majagual-Los Cacaos	M1	Impure marble: Cc+Dol+Qtz+Phg1+Chl1+Ab+Lw; Metapelite: Qtz+Phg1+Chl1+Lw+Cc	D1: P=3-6 kbar and T<300°C (b, f); LG-UG
	M2	Impure marble: Cc+Dol+Qtz+Phg2+Chl2+Ab; Metapelite: Qtz+Phg2+Chl2+Ab+Sph+Cc	
Punta Balandra	M1	Metapelite: Qtz+Phg1+Chl1+Grt+Ctd+Lw+Rt+Pg1	D1: P=10/12-16/20 kbar and T>430-480°C (b, f)
		Impure marble: Cc/Arag+Dol+Grt+Qtz+Phg1+Chl1+Pg1+Lw	D1:P>8-11 kbar and T=500-600°C (d, f)
		Metabasite: Grt+Omp+Phg1+Chl1+NaAmph1+Lw+Rt+Pg1 (b, c, d)	D1: P=13±2 kbar and T=450±70°C (b, c, e, f); UB-E
		Metabasite in mélange: Grt+Omp+Phg1+Rt (d)	D1: P=22-24 kbar and T=610–625°C (d, f)
	M2	Metabasite: Ep+Clz+Phg2+Chl2+NaAmph2+Pg2+Cc/Arag+Rt+Sp h+Ilm (d)	D2: P=10-16 kbar and T=400-550°C (d, f)
	M3	Metabasite: Ep+Clz+Phg3+Chl3+NaAmph2+Cc+Sph+Ilm (d)	Late D2, D3: P=5-10 kbar and T=300-400°C (d, f)
Santa Bárbara Schists (uppermost structural levels)	M1	Metapelite: Qtz+Phg1+Chl1+Mn- Grt+Ctd+Lw+Pg1+Rt+Sph	D1: P=8-12 kbar and T=300-450°C (b, f)
		Impure marble: Cc/Arag+Dol+FeGln+Qtz+Phg1+Chl1+Pg1+Lw	UB (f)
		Metabasite: FeGln+Ep+Phg1+Chl1+Lw+Rt+Sph+Pg1 (b, d)	D1: P=7,5±2 kbar and T=320±80°C (c, f)
	M2	Metapelite: Qtz+Phg2+Pg2+Sph+Ep+Ab+Bt+Hem	D2: LB to UG (f)
		Impure marble and calcschist: Cc/Arag+Dol+Qtz+Phg2 +Chl2+Pg2+Ep+Bt	(f)
		Metabasite: Act+NaCaAmph+Ep+Phg2+Chl2+Sph+Pg2 (b, d)	(f)
upper and lower levels	M1	Metapelite: Qtz+Phg1+Chl1+Fe- MgCar+Lw+Ab+Pg1 +Sph+Hem+Ilm	D1: P=4-8 kbar and T=250-350 (b, f)
		Impure marble: Cc/Arag+Dol+Qtz+Phg1+Chl1+Pg1+Lw+Sph	(f) LB
		Metabasite: Act+Phg1+Chl1+Lw+Ab+Pmp+Sph (b, d)	(b, d, f)
	M2	Metapelite: Qtz+Phg2+Pg2+Sph+Ab+Hem	D2: UG to LG
Rincón Marbles	M1	Impure marble: Cc+Dol+Qtz+Phg1+Chl1+Lw+Sph	D1: UB to LB-UG (f)
		Metapelite: Qtz+Phg1+Chl1+Lw+Ab+Sph+Hem	(f)
		Metabasite: Act+Phg1+Chl1+Lw+Ab+Pmp+Sph	(b, d, f)
Playa Colorado	M1	Metapelite: Qtz+Phg1+Chl1+Lw+Ab+Hem	D1: UG-LG (f)

(a) Mineral abbreviations after Bucher and Frey (2002), except for Fe-Mg carpholite (Car); (b) Joyce (1991).
(c) Gonçalves et al. (2000) ; (d) Escuder-Viruete et al. (2009); (e) Sorensen et al. (1997); (f) Escuder-Viruete (2008a, b).
Metamorphic facies: LG, lower greenschist; UG, upper greenschist; LB, lower blueschist; UB, upper blueschist; E, eclogites.

4.1. D1 deformation: isoclinal folding

The first recognizable deformation phase, D1, is characterized by mesoscopic rootless isoclinal and intrafolial fold hinges. In the Santa Bárbara and Punta Balandra nappes, these folds are rarely of more than several decimeters in size. D1 deformed primary sedimentary fabrics S0, e.g. marble-calcschist alternances, and early metamorphic veins or segregations of quartz and calcite, which often contain fibers of Fe–Mg carpholite or their pseudomorphs. Intense deformation in the course of later events, especially during the ductile D2 event, has obscured or entirely destroyed most of the D1 folds, as well as an S1 foliation, particularly in the upper structural levels of the Samaná complex. Some lithologies, however, have preserved an S1 fabric, mainly caused by competence contrasts. These include the marbles of the lower structural nappes, as can be seen on El Frontón and Loma Atravesada areas of the Rincón nappe, where the dominant foliation in the marbles, S1, is folded by a train of large-scale D2 folds (Fig. 3). Due to the scarcity and poor preservation of D1 folds, there is no means to quantify a transport direction related to D1.

At microscopic scale, much of the metapelite, calcschist and marble of the Santa Bárbara, Rincón and Playa Colorada nappes have a folded S1 foliation within S2 microlithons (Fig. 7). S1 is defined by the M1 blueschist mineral assemblage chlorite + phengite + quartz ± carpholite± chloritoid ± paragonite in Al-rich metapelites, lawsonite + chlorite + phengite + quartz+calcite ± paragonite in Ca-rich schists, and pumpellyte, lawsonite or glaucophane-bering assemblages in metabasites. In the Punta Balandra metapelites and calcschists, lawsonite, chloritoid and garnet porphyroblasts grew during M1 (Fig. 7b, c). In these rocks, idioblastic garnets (up to 5 mm diameter) preserve cores with sigmoidal and snow-ball inclusion trails of S1 quartz, lawsonite, chloritoid, rutile and graphite that often are surrounded by clinozoisite-bearing rims. Fine-grained clusters of clinozoisite, paragonite and phengite form rectangular pseudomorphs after S1 lawsonite in the core and inner rim of garnet that grades to an inclusion-poor outer rim. Similar microtextures occur in some interlayered eclogitic mafic lenses, where garnet porphyroblasts are texturally zoned from Mn-rich cores that have sigmoidal inclusions of S1 lawsonite and omphacite, to Fe-rich inner rims that include epidote and grades to an inclusion-poor outer rim (Escuder-Viruete and Pérez-Estaún, 2006).

4.2. D2 deformation

4.2.1. D2 tight to isoclinal folding

Tight to isoclinal folds and thrusts formed by the D2 deformation are the most prominent macrostructures in the Samaná complex. Towards upper structural levels the strain intensity of D2 folding and associated shearing of fold-limbs increase. In the NE sector of the complex, the Rincón Marbles nappe is internally folded at a several-hundred-meter scale by a large train of D2 folds. This train comprises several asymmetrical antiforms and synforms with WSW–ENE axes and NE vergence (Fig. 6f), which

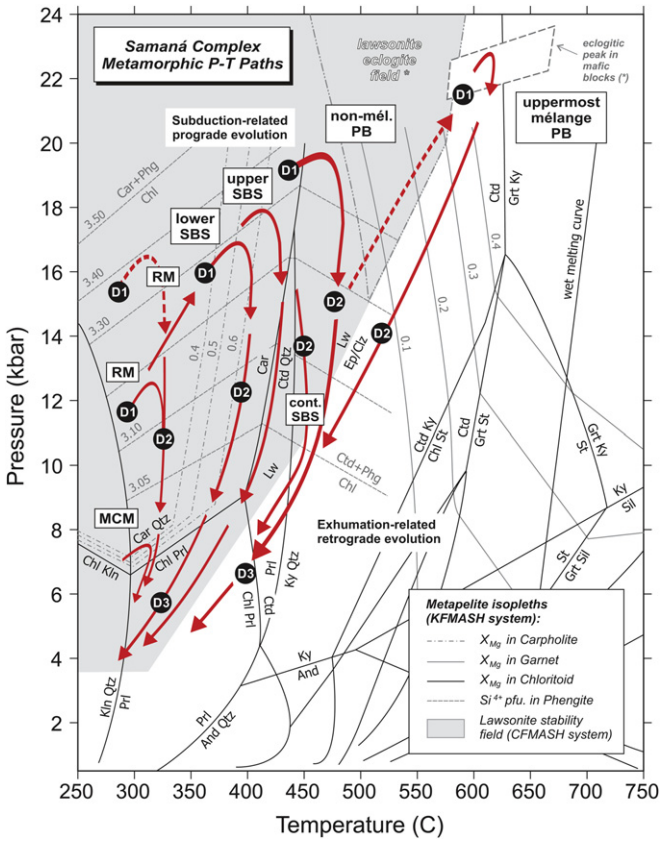

Fig. 5. Generalized P-T paths for the different metamorphic nappes in the Samaná complex (Escuder-Viruete et al., 2011). The P–T path for uppermost mélange part of the Punta Balandra nappe was deduced from mafic eclogite blocks by Escuder-Viruete and Pérez-Estaún (2006), which crossing a lawsonite-eclogite field (*) defined for these mafic compositions. Encircled numbers correspond with metamorphic events described in the text and Table 2. The figure also include as reference the petrogenetic grid for metapelites for a temperature range from 250 to 750 °C in the KFMASH (K_2O–FeO–MgO–Al_2O_3–SiO2–H_2O) system, where the mineral assemblages are strongly temperature-controlled. The appearance of high-P assemblages with Fe–Mg carpholite or chloritoid delimits the low-T domain from the middle-T one at around 400 °C. The exact temperature limit depends on rock and mineral chemistry. In the CFMASH (CaO–FeO–MgO–Al_2O_3–SiO2–H_2O) system, lawsonite is the main stable mineral under low-T conditions, sometimes coexisting with Fe–Mg carpholite. Grids drawn after Spear (1993), Vidal et al. (1992), Bousquet et al. (2002) and Rimmelé et al. (2005), as well as own calculations of mineral isopleths using the *Theriak-Domino* software (details for the used thermodynamic data base and solution models are in the Appendix 3). Other reactions are: 5Qtz + Chl+2Ms+2W = 3Car + 2Phg and 2Ms + Chl+2Qtz = W+2Phg+3Ctd (Phg stands here for the celadonite activity in mica). Mineral abbreviations are from Bucher and Frey (2002) except for Fe–Mg carpholite (Car). Nappes: RM = Rincón Marbles; SBS = Santa Bárbara Schists; PB = Punta Balandra (non-mélange and mélange parts); and MCM = Majagual-Los Cacaos Marble.

show long normal limbs and short reversed limbs, some separated by small thrusts (III–III' cross section, Fig. 3). Development of a macroscopically visible S2 schistosity is mainly confined to the hinge zone of this fold structure and ductile thrust surfaces (see below). In the Santa Bárbara Schist, several kilometer- to hectometer-scale folds developed in marble intercalations are D2 structures (IV–IV' cross section, Fig. 4). These D2 folds re-fold S1 and are intrafolial with respect to the main S2 foliation. Most of the measured folds in the Punta Balandra nappe are preserved only as isolated fold hinges, so that a distinction between D1 and D2 folds was not always possible.

D2 deformation is responsible for the SW to SSW-dipping S2 dominant regional foliation observed over most of the Samaná complex (Fig. 4). Except some marbles of the Rincón nappe, the S2 foliation is the penetrative fabric in almost all lithologies and in all scales. In the Santa Bárbara metapelites and calcschists, the S2 foliation is defined by M2 oriented growth of chlorite, phengite, paragonite, quartz and, in part, calcite/dolomite, albite, biotite, glaucophane, actinolite, rutile and titanite, or a differentiated layering of quartz and sheet silicates on a 0.1–2.5 mm-scale. In the uppermost structural levels of this nappe, the late-M2 blastesis of coarse-grained elongate albite poikiloblasts is ubiquitous. They contain inclusion trails comprising S2 phengite, paragonite, glaucophane, chorite quartz and graphite, with or without biotite and clinozoisite. Other D2 typical structures are WNW–ESE trending asymmetrical, isoclinal and often rootless similar-style folds and sheath folds, boudinage of S2 foliation, syn-M2 veins of quartz and/or calcite, and penetrative shear bands. In micaschists, S2 is often an S–C mylonitic fabric, where the angles between the S and C planes are lower than 30°. The L2 mineral and stretching lineation visible on the S2, S and C planes is dominantly ENE–WSW to E–W, with a plunge to the NW and SE that is generally less than 30° (Fig. 8). It is marked by elongated quartz aggregates and rods, preferred orientation of phengite flakes, oriented white mica-chlorite associations replacing carpholite crystals, and asymmetric strain shadows developed around syn-D2 lawsonite, epidote and titanite porphyroblasts. The metapelites of the Punta Balandra unit contain quartz, clinozoisite, and garnet porphyroblasts enveloped by combinations of S2 phengite, paragonite, chlorite, glaucophane, rutile, titanite and calcite, as well as clinozoisite-paragonite rhomboidal pseudomorphs after lawsonite. Lawsonite is never observed external to garnet. All these microstructures point to decreasing high-P metamorphic conditions during D2 (from M1 eclogite and upper blueschist to M2 blueschist and greenschist-facies).

Kinematic indicators associated with S2 are asymmetric strain shadows around garnet, titanite, glaucophane, chloritoid, calcite and albite, and the asymmetry of D2 isoclinal folds and boudins, S–C fabrics and oblique grain-shape fabrics in quartz and calcite aggregates. At map-scale (Fig. 10), they consistently indicate a top-to-the-NE and E shear sense during D2, particularly above the Majagual-Los Cacaos and Punta Balandra basal thrusts, where the D2 tectonites are mylonitic.

4.2.2. D2 thrusting

Prominent structural features in the metamorphic complex are thrusts. They are defined by lithological differences and a gradual increase of D2 simple shear and penetrative retrograde lower blueschist/greenschist overprint towards the contacts. Calcschists and impure dolomitic marbles of the Santa Bárbara Schist nappe immediately below the Punta Balandra basal thrust preserved D2 structures. These are an S2 foliation made up by phengite, chlorite, ferro-glaucophane, winchite, epidote, quartz and calcite, and an NNW to ENE-trending stretching lineation expressed by phengite and Na-amphibole alignment. The penetrative S2-L2 fabric in micaschists immediately above the Punta Balandra basal thrust has the same orientation (Fig. 8). In these rocks, quartz ± clinozoisite aggregates defining a stretching lineation and garnet porphyroblasts preserved asymmetric internal fabrics indicating a top-to-the-NE sense of shear during D2. At map-scale (Fig. 4), the orientation of this thust contact is sub-parallel to the regional foliation S2 and the axial planes of macroscopic D2 folds in the Santa Bárbara nappe. Metamorphic grade across this and other mapped thrust planes, as the Santa Bárbara and Playa Colorada basal thrusts, shows no very sharp boundaries. Furthermore, the D2 structural inventories north and south of the thrusts are generally identical. Therefore, this ductile thrusting is interpreted as a final stage of D2 horizontal shortening, which took place whenever shortening exceeded a degree of what could be accommodated by the D2 folding. The above-mentioned observations on metamorphic grade and structural

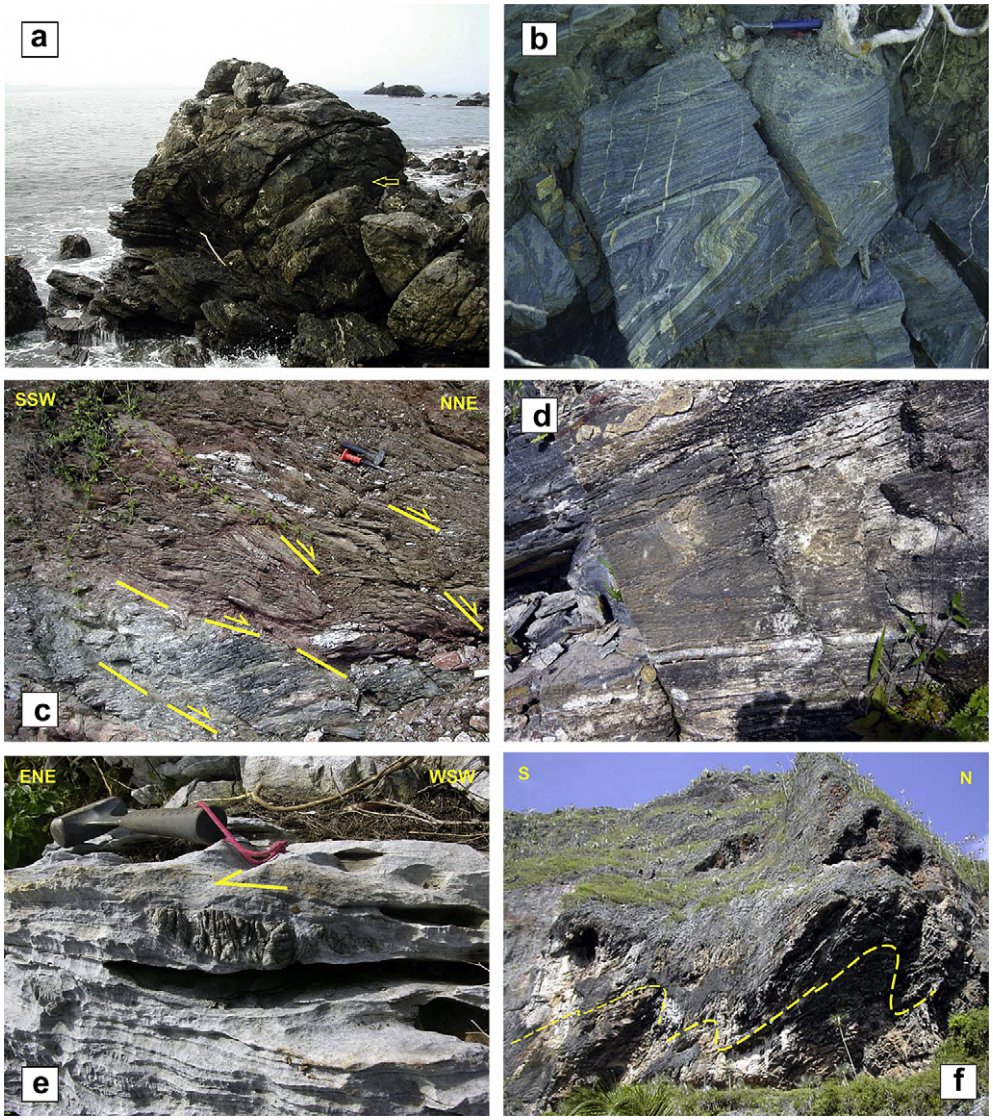

Fig. 6. Field aspect of D2 and D4 structures in the Samaná complex: (a) Mafic eclogite ellipsoidal block (about 6 m width; arrow) surrounded by strongly foliated (S2) metasediments, upper Punta Balandra nappe; (b) Banded mafic blueschists affected by ENE-WSW-trending asymmetric, isoclinal and rootless similar-style D2 folds. Axial planar fabrics in folds (S2) contain syntectonic epidote-blueschists facies mineral assemblages; (c) System of dm- to cm-spaced D4 ductile and ductile-brittle shears in micaschists of the Santa Bárbara Schists nappe, showing a top-to-the-NNE normal sense of desplacement; (d) Isoclinal D2 fold displayed by a marble-calcschist compositional alternance (S0/S1) in the Santa Bárbara schists nappe (width of field 1 m); (e) Rotated siliceous marble asymmetrical clast in foliated (S2) calcitic marble above the Santa Bárbara Schists basal thrust indicating top-to-the-E sense of shear; (f) Marbles folded at hundred-meter scale by a train of asymmetrical D2 folds with WSW-ENE axes and NE vergence, El Frontón area, Rincón Marbles nappe (width of field about 350 m).

features indicate that, after the cessation of crustal shortening, no major displacements along the nappe stack basal contacts took place.

An exception to this distribution is the Majagual-Los Cacaos basal thrust, which cuts the Punta Balandra basal thrust and localizes across a jump in the P–T metamorphic conditions (see bellow). This structural contact can be traced across southern Samaná Peninsula, running E-W from Punta Balandra to Santa Bárbara de Samaná (Fig. 2). It is regarded as a thrust because it juxtaposes a tectonic ductile mélange of sedimentary, mafic and ultramafic rocks against pure marbles and calcschists, an association that is not likely to be primary. To the west, the Majagual-Los Cacaos basal thrust cross-cut the S2 traces at a small angle (Fig. 2) and at outcrop scale show signs of brittle overprint. This overprint is caused by a poorly defined later stage normal sense reactivation.

Impure calcitic marbles of the Majagual-Los Cacaos nappe immediately over the basal thrust preserved in part D2 structures. These are an SE-dipping S2 foliation made up by phengite, chlorite, quartz, calcite and opaques and an ENE to E-trending stretching lineation expressed by phengite and quartz alignment. The asymmetry of phengite mica-fish and of the internal fabric in quartz aggregates suggests a top-to-the-ENE sense of shear during D2. However, D2 structures are strongly overprinted by D4 shear and faults. In turn, the contact between the Majagual-Los Cacaos and the Punta Balandra nappes is characterized in the field by a distinct, dark and planar, <50-cm-thick layer of severely cataclastically reworked metapelite and marble. In this layer, kinematic indicators are calcite porphyroclasts, Riedel planes and P foliations, which yielded a normal top-to-the WSW to SW, sense of shear. Alteration during cataclasis was associated with pronounced influx of fluids,

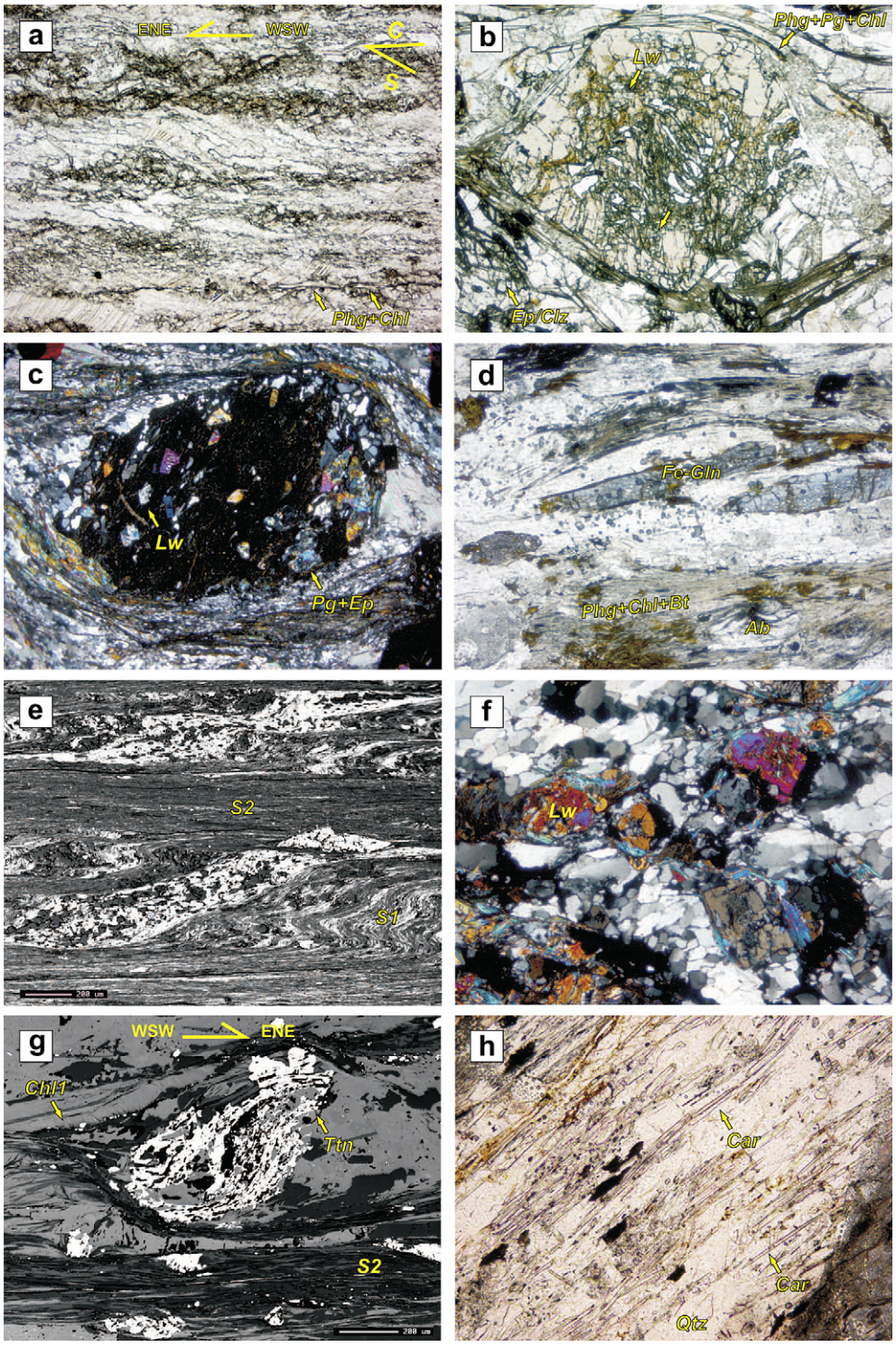

Fig. 7. Microphotographs of D2 structures. (a) Polycrystalline calcite aggregate dynamically recrystallized during D2 deformation. Elongate grains of calcite define an oblique shape fabric respect to the phengite + chlorite alignement (S2 foliation; arrows), indicating a top-to-the-ENE sense of shear. Majagual-Los Cacaos Marbles nappe. PPL, width of field = 1.2 mm; (b) Idioblastic garnet (3.5 mm in diameter) zoned with respect to mineral inclusions, showing sigmoidal inclusions trails of S1 quartz, lawsonite, chloritoid, rutile and graphite in the cores, enclosed by a inclusion-poor outer rim. Garnet porphyroblasts is enveloped by S2 phengite, paragonite, chlorite, rutile, titanite and calcite. Calcschits of the Punta Balandra nappe. PPL, width of field = 5 mm; (c) Syn-D2 garnet porphyroblast with lawsonite inclusions in the core and epidote-paragonite rhomboidal pseudomorphs after lawsonite in the rim. Pelitic schits of the Punta Balandra nappe. CPL, width of field = 5 mm; (d) Coarse-grained ferro-glaucophane elongated with S2 phengite, chlorite and quartz. Note late-D2 growth of albite and biotite. Calcschists of the uppermost Santa Bárbara Schists nappe PPL, width of field = 5 mm; (e) BSE (back-scattered electron) image of a poor differentiated subhorizontal crenulation cleavage (S2) deforming quartz-calcite aggregates and a finely spaced previous cleavage (S1). Calcschists of the Santa Bárbara Schists nappe; (f) Idioblastic lawsonite porphyroblats in quartz-rich schists. Santa Bárbara Schists nappe. CPL, width of field = 1.2 mm; (g) BSE image of titanite porphyroblasts with sigmoidal inclusions trails of S2 quartz, chlorite, phengite, and opaques, which are continous with the external S2 matrix foliation. Note relics of pre-S2 high-P chlorite (Chl1). Schists of the lower structural levels of Santa Bárbara nappe; and (h) Quartz-hosted carpholite hair-like fibers (arrows). Lower structural levels of Santa Bárbara nappe. PPL. PPL and CPL = plane and crossed polarized light, respectively.

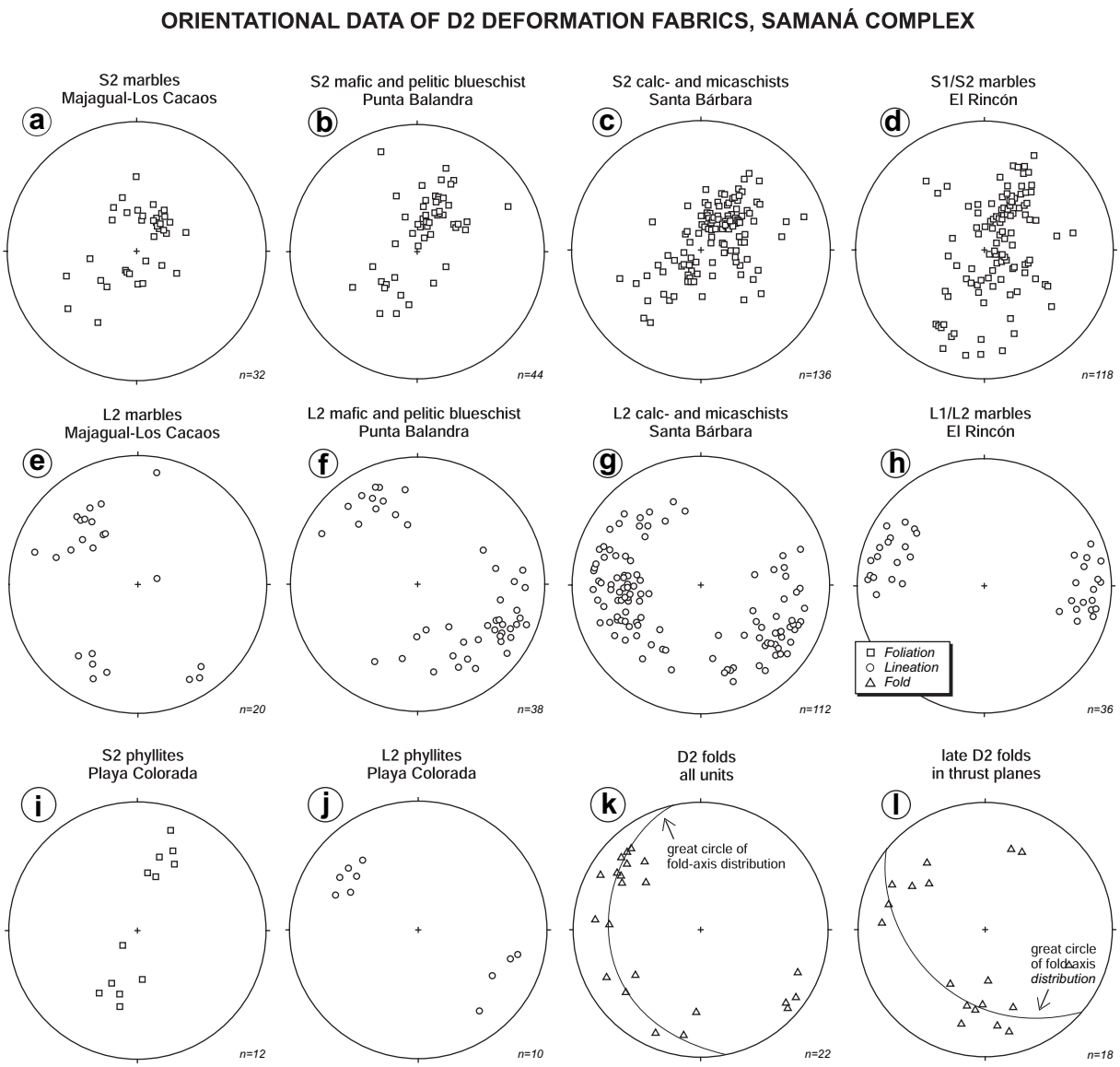

Fig. 8. Orientational data (lower-hemisphere equal-angle projections) of D1 and D2 deformation elements.

which caused the development of phyllosilicate and clay minerals and produced the dark matrix.

4.3. D3 deformation: kink folding and crenulation

D3 was a discontinuous deformation, much less penetrative than the previous D2. D3 structures are upright to slightly NE-vergent open to tight folds, often of kink geometry, centimetric to kilometric in size and with NW-SE to WNW–ESE axes. These structures are restricted to narrow D3 deformation bands, often no more than outcrop size, and preferentially developed in the Santa Bárbara Schist nappe. In the Rincón and Majagual-Los Cacaos nappes, D3 deformation only undulate the S2 planes. The D3 folding was cylindrical, as is indicated by the arrangement of the poles of S2 along a subvertical great circle in stereographic projection; the pole (N297°E/06°NW) to this great circle coincides with the general direction of D3 folds axes on the macroscale (average N308°E/14°NW; Fig. 9b).

On outcrop scale, D3 folds are characterized by fold-axis-parallel crenulation lineation (L3) sometimes associated with a non-pervasive, subvertical spaced cleavage (S3; Fig. 9a). On the regional scale, the major D3 folds define a set of subvertical or moderately NE-vergent antiforms and synforms (Fig. 3), which fold the S2 foliation, the contacts between structural units and the M2 metamorphic isograds. In thin section, phengite and chlorite deformed by D3 are bent with minor or without M3 recrystallization in the fold hinges, and Fe–Mg silicates were partially reemplaced by chlorite, indicating that D3 took place under ductile to ductile-brittle conditions. Therefore D3 is placed at a late stage of the retrograde M3 greenschist-facies overprint, probably at temperatures of ~300 °C.

4.4. D4 deformation: ductile-brittle normal shears

The D4 structures are ductile-brittle normal shears and associated subhorizontal folding. These discontinuous structures were spatially very limited and not accompanied by extensive recrystallization and grain growth. Fabrics associated with D4 are therefore not pervasively developed. The D4 structures overprint the D3 folds and occur preferentially in the Punta Balandra and

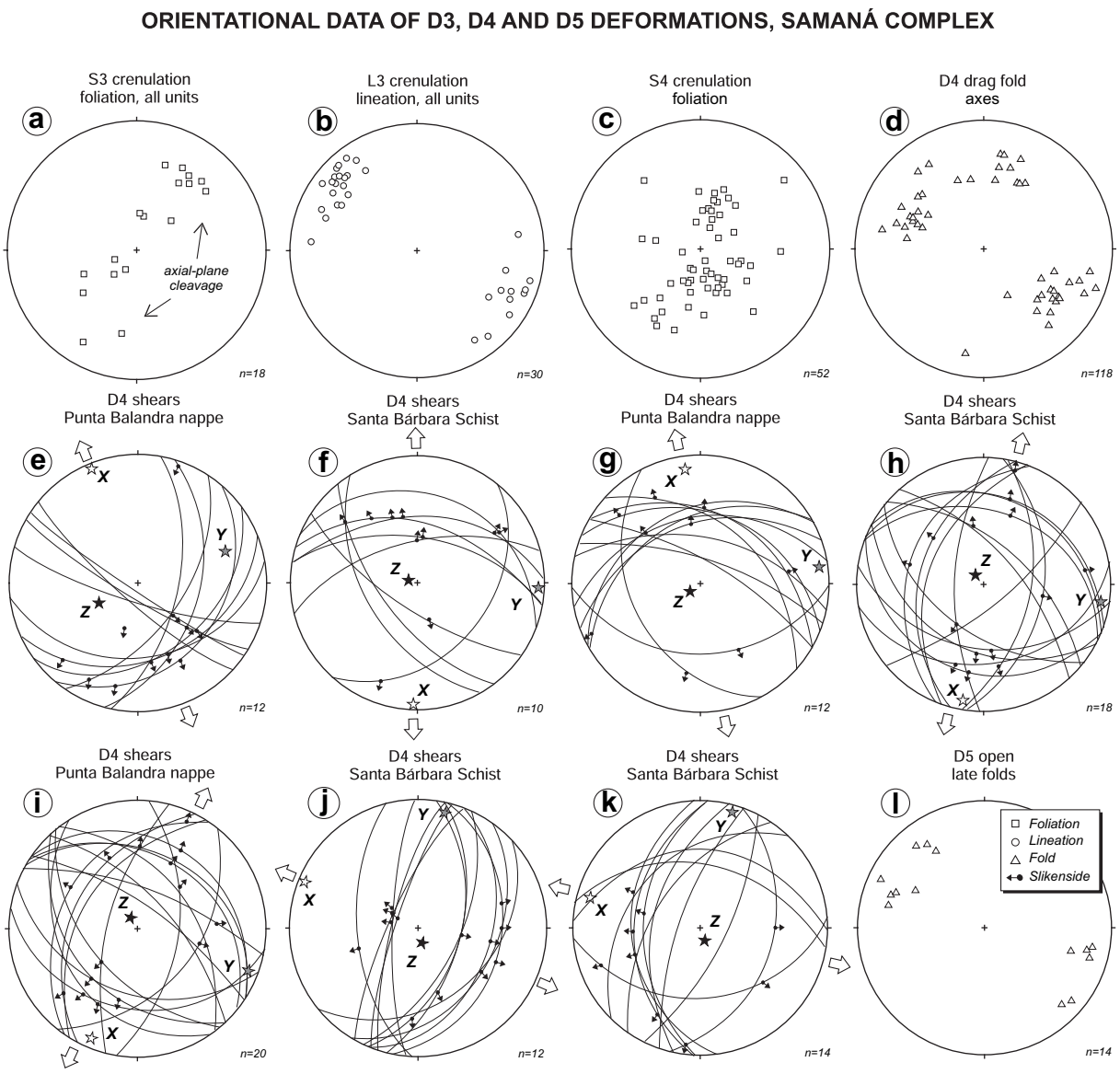

Fig. 9. Orientational data (lower-hemisphere equal-angle projections) of D3, D4 and D5 deformation elements. For D4 ductile-brittle shears and faults, the orientation of each shear and fault is illustrated by great circles; the arrows indicate the relative sense of slip as deduced from asymmetry of kinematic indicators and slickenside measurements on the planes; principal strain axes are shown; the large open arrows indicate the deduced extension direction.

Santa Bárbara nappes, which indicate an increase in intensity of D4 towards the upper structural levels of the complex. The ductile-brittle shears and faults occur in two main families (Fig. 9): the N–S to NNE–SSW, with dips between 25 and 80° towards the W and E; and the W–E to NW–SE, generally with low to mid-angle dip (<60°) toward the NE and NE, and apparently more common in the Punta Balandra nappe. In outcrops, D4 shear systems look like decimeter to meter-scale extensional crenulation cleavage, in which the S2 curves into the D4 shear plane thus indicating normal displacement. On a lesser scale, the shear bands only developed in rocks with a strong planar anisotropy, as micaschist, and where the synchronous crystallization of (little-deformed) quartz and/or calcite-bearing veins often occurs. A W-E to NW-SE and NNE-SSW to NNW-SSE trending stretching lineation (L4), marked on small quartz grains, respectively for each family, is sometimes visible on such planes. In thin section, the older S2 mica foliation is crenulated and in part kinked, and irregular or stylolitic solution-transfer seams marked by concentration of opaques, sericite and chlorite form a spaced S4 cleavage. The seams wrap around and thus post-date M2 albite porphyroblasts.

In the metasediments asymmetrical D4 folds of angular geometry with subhorizontal axial surfaces also occur. They are often organized into cascades, without any obvious axial planar fabrics, and spatially limited by D4 shear planes. The orientation of the axes is variable, from N–S to NW–SE (Fig. 9d), and the asymmetry of drag folds indicate essentially normal movements, often with axial planes are occupied by ductile-brittle and cataclastic fault zones. The orientation of the normal shear bands and faults in conjugate systems is extremely variable. In favorable cases the mutual displacements of conjugate systems measured indicates an approximate subhorizontal NNE–SSE to NNW–SSE or NW–SE extension direction, subperpendicular to the drag fold axes (Fig. 9e, k).

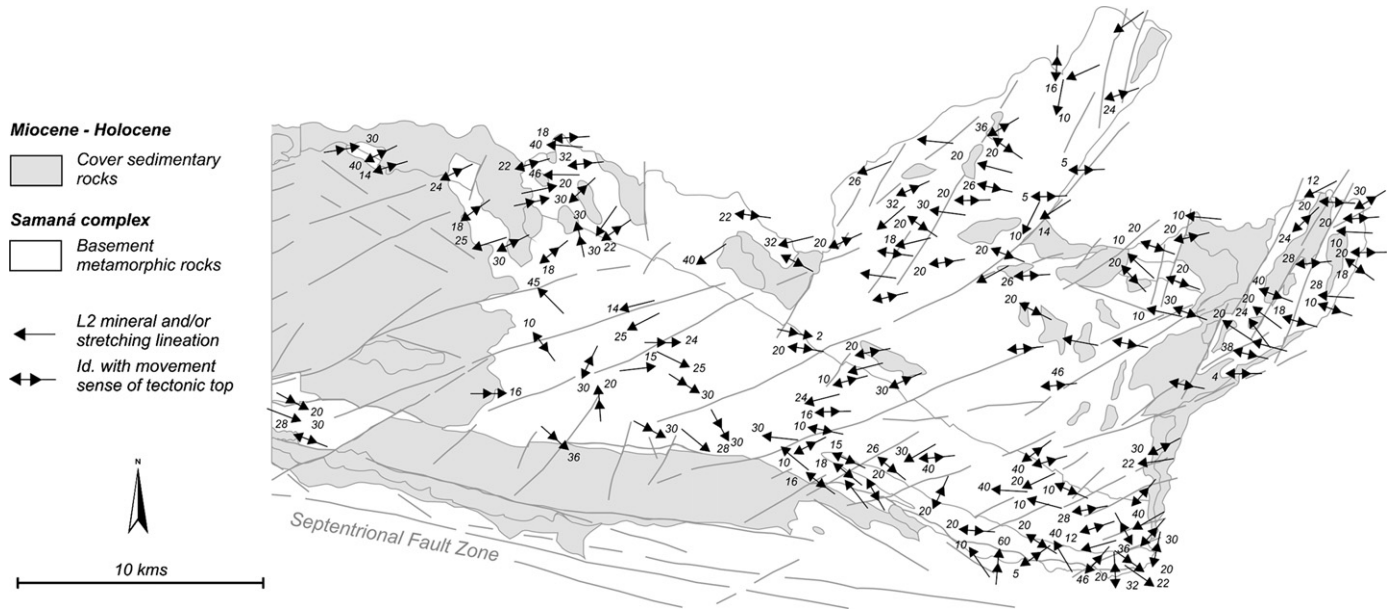

Fig. 10. Map of L2 mineral and stretching lineation with indication of movement sense of tectonic top deduced from kinematic indicators at meso- and microscale. In occasions, each symbol represents mean of between 2 and 14 measurements in the vicinity of symbol. In spite of folding of S2-L2 fabrics by the later D3 deformation, a general top-to-the-NE/ESE sense of shear for D2 deformation can be deduced.

4.5. D5 deformation: later stage postmetamorphic deformations

The rocks of Samana complex are affected by a number of late brittle deformation phases post-dating greenschist-facies overprint. Quite often, brittle deformation has considerable influence on the geometry of the whole structural succession. A common characteristic for all late events is that they lead to brittle behavior in marbles. Assuming a geologically realistic strain rate of 10^{-15} s^{-1} (Heard and Raleigh, 1972), calcite reacts brittly below 250 °C, indicating that these deformation events either formed part of a late stage of the metamorphic evolution or reflect final emplacement of the rocks to their present-day position. The brittle structures identified are: (1) left-lateral strike-slip faults and (2) late normal faults. Constraints on their relative and absolute age are briefly discussed below.

The Septentrional Fault Zone produces a 1–3 km width corridor of transpressional brittle deformation in the south coast of Samaná Peninsula. This corridor affects the metamorphic complex and the Tertiary and Pleistocene sedimentary rocks. Considered as a whole, the Septentrional Fault Zone originates the net elevation of the septentrional block of the Samaná Peninsula (and tilted ~8° to the N) and the sinking of the meridional block below the Samaná Bay. Related to this event is a system of ENE-WSW to W-E-trending, brittle left-lateral strike-slip faults. Tectonic stress could be identified as roughly NE–SW directed, as derived from geometric relationships between the main strike-slip fault plane and associated Riedel shears. The last recorded deformation event is characterized by the development of steep normal faults cutting all other structures to the east of Samaná Peninsula. Recorded vertical displacements along the faults range between 10 and 100 m. The most prominent strike direction of steep normal faults is NNE-SSW (Fig. 2). This tendency is also observed in a statistical analysis of measured small-scale normal faults (Escuder-Viruete, 2008a).

5. $^{40}Ar/^{39}Ar$ geochronology: samples and results

Mafic eclogites of the Punta Balandra nappe and metasediments of the Punta Balandra, Santa Bárbara and Rincón nappes were selected for dating by $^{40}Ar/^{39}Ar$ method (Fig. 11). Samples show a strong mineral plano-linear S2 foliation defined by 0.5–10 mm long glaucophane nematoblasts and/or phengite lepidoblasts consistent with the simultaneity of D2 ductile deformation and high-P blueschist facies metamorphism. Map in Fig. 2 shows the sample locations. Analytical procedures are in Appendix 1 and results are reported in Appendix 2. All ages are quoted at the 2σ level of uncertainty.

Fig. 11 also includes the ages obtained in two mafic eclogite blocks from the Punta Balandra nappe by Escuder-Viruete and Pérez-Estaún (2004), which allow comparing the different $^{40}Ar/^{39}Ar$ age spectra in the later discussion. These eclogite blocks are enclosed in the uppermost mélange of the nappe and surrounded by foliated epidote-glaucophane mafic schists. Mafic protoliths are N-MORB and IAT-like Fe-Ti-rich gabbros with a $(\epsilon_{Nd})_i = +7.2$ (t = 86 Ma) value, suggesting derivation from depleted mantle sources (for details see Escuder-Viruete, 2008b). Sample 2JE74 is a phengite-bearing granoblastic eclogite collected in the core of the block. It yielded $^{40}Ar/^{39}Ar$ glaucophane and phengite ages of 49.91 ± 0.29 Ma and of 36.30 ± 0.13 Ma, respectively. Sample 2JE80 is a blastomylonitic eclogite with minimal secondary recrystallization collected from a banded block. This rock yielded $^{40}Ar/^{39}Ar$ glaucophane and phengite ages of 80.86 ± 0.51 Ma and 33.68 ± 0.47 Ma, respectively.

Sample 4JE94 is a coarse-grained banded eclogite characterized by alternating garnet-rich and omphacite-rich bands, enclosed in strongly foliated (S2) epidote-glaucophane mafic schists. It was collected in the non-mélange part of the Punta Balandra nappe at Cayo Grepin outcrop. Mafic protoliths are IAT-like tholeiitic Fe–Ti gabbros. The obtained glaucophane plateau age is 33.52 ± 0.96 Ma (MSWD = 1.6) for six steps (3–8) and 90.6% of the ^{39}Ar released. The isochron correlation age on these six points is 35.0 ± 1.4 Ma (MSWD = 0.14), with a $^{40}Ar–^{36}Ar$ intercept at 282 ± 11, which is close to the atmospheric value of 295.5.

Sample 4JE125 is a semi-pelitic metasediment with a strong S2-L2 fabric from the non-mélange Punta Balandra nappe at Puerto Viejo. The microstructure contains garnet porphyroblasts (up to 10 mm in diameter) with lawsonite inclusions enveloped by

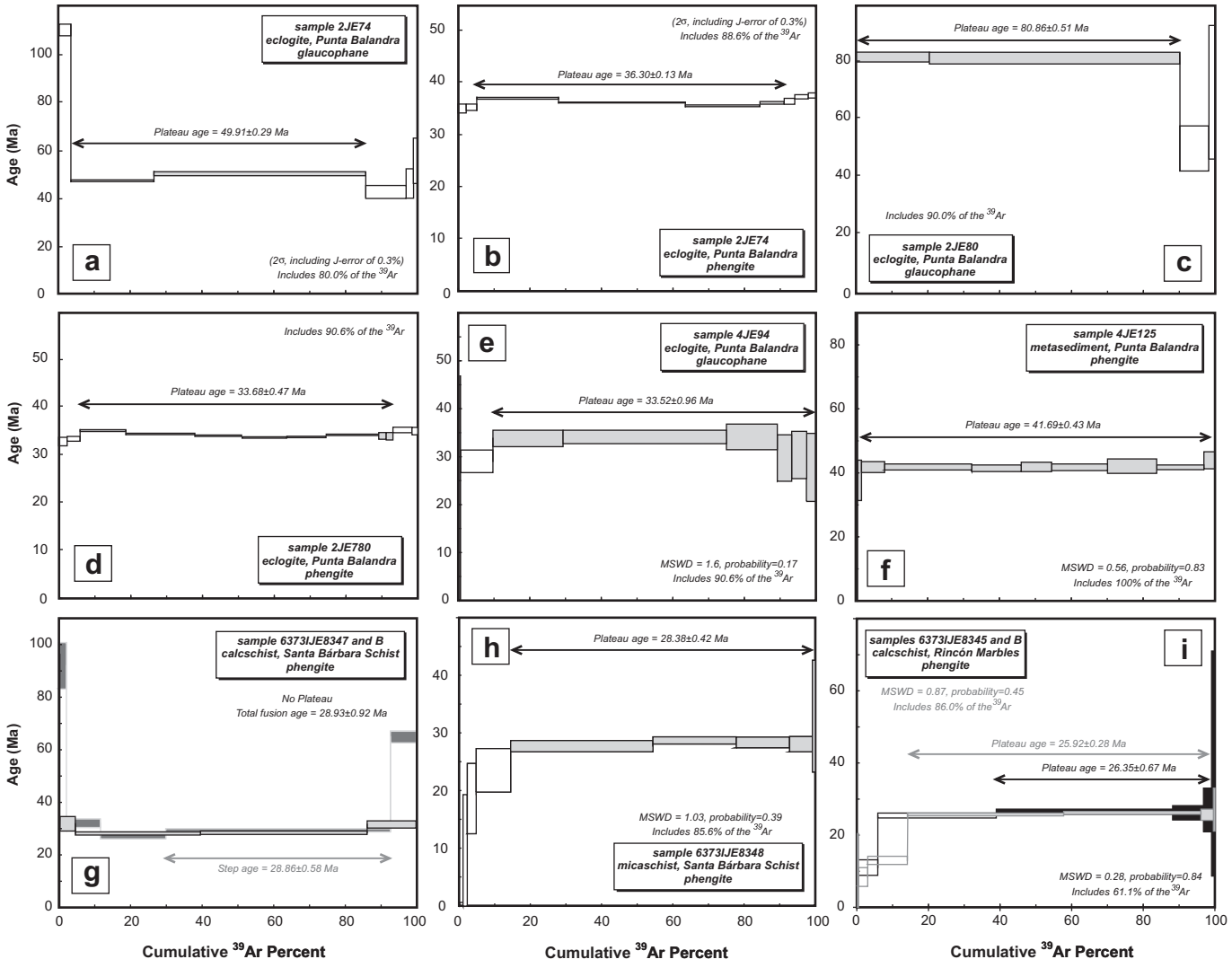

Fig. 11. The $^{40}Ar/^{39}Ar$ spectrum of galucophane and phengite from mafic eclogite and blueschists metasediments of the Samaná complex. The plateau ages were calculated following techniques described in Appendix 1. A summary of $^{40}Ar–^{39}Ar$ incremental heating experiments is in Appendix 2. See text for discussion.

combinations of S2 phengite, paragonite, clinozoisite, rutile, titanite and quartz. The obtained phengite plateau age is 41.69 ± 0.43 Ma (MSWD = 0.56) for all steps (10) and 100% of the ^{39}Ar released. The isochron correlation age on these ten points is 41.53 ± 0.83 Ma (MSWD = 0.60), with a $^{40}Ar–^{36}Ar$ intercept at 297.9 ± 8.5.

Sample 6373IJE8347 is a medium to coarse-grained calcschist with an intense S2 foliation defined by alternating quartz-rich and calcite-rich bands. It was collected in the Santa Bárbara Schist nappe, near the tectonic contact with the overlying Punta Balandra nappe at Punta La Chiva. Under the microscope, the calcschist displays an S2 foliation defined by combinations of quartz, calcite, phengite, epidote and chlorite, with or without albite, glaucophane, rutile, titanite, clinozoisite and relict lawsonite. The obtained total fusion age (no plateau) in phengite is 28.93 ± 0.92 Ma and the normal isochron age is 28.3 ± 1.9 Ma (MSWD = 3.8). The inverse isochron age on five steps is 29.3 ± 3.1 Ma (MSWD = 6.9), with a $^{40}Ar–^{36}Ar$ intercept at 297.0 ± 40, within error of the total fusion age. A similar sample from the same outcrop (6373IJE8347B) yields a phengite total fusion age of 32.80 ± 0.64 Ma, but the age for a step (4) and for the 63% of the ^{39}Ar released is 28.86 ± 0.58 Ma.

Sample 6373IJE8348 is medium-grained schist with a strong S2-L2 fabric, collected in the Santa Bárbara Schist nappe at El Palmito Play, north of Santa Bárbara locality. The S2 microstructure is defined by aligneated quartz, calcite, phengite, chlorite and lawsonite (relicts and pseudomorphs). The obtained phengite plateau age is 28.38 ± 0.42 Ma (MSWD = 1.03) for five steps (5–9) and 85.6% of the ^{39}Ar released. For all steps, the normal isochron age yields 27.78 ± 0.46 Ma (MSWD = 0.87) and the inverse isochron age is 28.85 ± 0.46 Ma (MSWD = 0.82), with a $^{40}Ar–^{36}Ar$ intercept at 270.5 ± 7.4.

Sample 6373IJE8345 is a fine-grained calcschist comprising combinations of aligned S2 phengite, calcite, quartz, chlorite, titanite, albite, lawsonite and graphite. It was collected in the Rincón Marbles at Puerto El Frontón. The obtained phengite plateau age is 26.35 ± 0.67 Ma (MSWD = 0.28) for four steps (3–6) and 61.1% of the ^{39}Ar released. The isochron correlation age on these five points is 25.72 ± 0.51 Ma (MSWD = 1.6), with a $^{40}Ar–^{36}Ar$ intercept at 301.0 ± 12. A similar sample from the same outcrop (6373IJE8345B) yields a phengite plateau age of 25.92 ± 0.28 Ma (MSWD = 0.87) for four steps (4–7) and 86% of the ^{39}Ar released.

6. Interpretations and discussion

6.1. $^{40}Ar/^{39}Ar$ ages interpretation

The group of obtained $^{40}Ar/^{39}Ar$ ages represents retrograde growth/cooling of sodic amphibole and white mica through the appropriate argon retention temperature of the mineral. Due to the syn-S2 growth of glaucophane in the foliated rinds of the eclogite blocks in the Punta Balandra nappe and the closure temperature of amphibole (525–450 °C) for cooling rates of 5–50 °C/Ma (McDougall and Harrison, 1999), the obtained $^{40}Ar/^{39}Ar$ plateau age in sample 4JE94 indicates D2 ductile deformation and cooling in the blueschist facies conditions at about 33 Ma (Late Eocene), during the retrograde P–T path of the unit. However, similar eclogite blocks enclosed in the mélange part of the Punta Balandra nappe yielded $^{40}Ar/^{39}Ar$ glaucophane ages of 80.86 ± 0.51 Ma (Campanian; 2JE80) and 49.91 ± 0.29 Ma (lowermost Eocene; 2JE74). Therefore, the $^{40}Ar/^{39}Ar$ glaucophane ages between 80 and 33 Ma recorded in the eclogites indicate a different exhumation history for the different blocks.

On the other hand, the Ar closure temperature for metamorphic white mica varies with composition but ranges from ~450 to 350 °C for cooling rates of 5–50 °C/Ma for grains with average diffusion dimensions of ~5.0 μm (McDougall and Harrison, 1999), which is larger than the mica grain-size from any sample in this study. $^{40}Ar/^{39}Ar$ analyses of phengite from the eclogite to blueschist facies metasediment (4JE125) of the non-mélange part of the Punta Balandra nappe, therefore, yield postmetamorphic-peak cooling ages at about 41 Ma. In addition, the eclogite blocks enclosed in the mélange yielded younger $^{40}Ar/^{39}Ar$ phengite cooling ages of 36.30 ± 0.13 Ma and 33.68 ± 0.47 Ma (Late Eocene). These ages are similar to the *in situ* $^{40}Ar/^{39}Ar$ laser-probe individual phengite ages between 48.9 ± 3.7 and 25.5 ± 2.5 Ma ($n = 48$; average 37.8 ± 2.6 Ma; MSWD = 13) reported by Catlos and Sorensen (2003) in similar eclogite blocks and their actinolite-rich metasomatic selvages, probably collected from the uppermost mélange-like structural levels of the Punta Balandra nappe.

In summary, the $^{40}Ar/^{39}Ar$ glaucophane and phengite ages between 80 and 33 Ma recorded in the Punta Balandra nappe, given that they record cooling over a temperature interval of 525–350 °C, indicate a relatively slow cooling, and suggest that the uppermost structural levels of the Punta Balandra nappe correspond to a true mélange zone in the sense of Cloos and Shreve (1988), Schwartz et al. (2000) or Gerya et al. (2002), for which each eclogitic block embedded in a metasedimentary or serpentinite-matrix records distinct P-T-t evolution. The tectonic implications are discussed below.

Lower peak metamorphic temperatures for the uppermost structural levels of the Santa Barbara Schists (400–450 °C) and for the Rincón Marbles (325 ± 25 °C) suggest that the metamorphic white micas in samples from these nappes grew at or below their closure temperature (at least 350–380 °C). Therefore, the total fusion age of 28.9 ± 0.9 Ma and the plateau ages of 28.4 ± 0.4 Ma and 26.35 ± 0.67 Ma obtained in syn-D2 phengites from samples JE8347, JE8348 and JE8345, respectively, most likely reflect the time of maximum prograde metamorphism for the Santa Barbara and the Rincón Marbles nappes. No detrital mica was observed in any thin section of both units, due to the very strong degree of deformation and recrystallization. In addition, the $^{40}Ar/^{39}Ar$ ages of the metamorphism in the Santa Bárbara Schists and the Rincón Marbles nappes are between them consistent and younger than the exhumation of the overlying Punta Balandra nappe, indicating that ductile thrusting and metamorphism of the southern margin of the North America plate (Bahamas Platform) was under way by 29–26 Ma (Early Oligocene). Exhumation of the high-pressure metamorphic rocks by Middle/Late Eocene to Early Oligocene time is consistent with the presence of metamorphic detritus, including blue amphiboles, in the turbidite syn-collisional basins of this age in the western Septentrional Cordillera (Draper Nagle, 1991).

6.2. Metamorphic P–T paths

In the Samaná complex, high-P metamorphic conditions are indicated by the presence of lawsonite in Ca-rich metapelites and calcschists, and Fe–Mg carpholite in Al-rich metapelites, marbles, albite-free pelitic schists, and quartz or calcite veins, which are index minerals in lawsonite blueschist facies metapelites (e.g. Goffé and Bousquet, 1997; Vidal et al., 1992; Bousquet et al., 1998; Rimmelé et al., 2003). In the uppermost structural levels of the Santa Bárbara nappe, lawsonite is replaced by pseudomorphic clinozoisite and white mica, with or without glaucophane, which corresponds to the transition between lawsonite blueschist and epidote-blueschits facies. Garnet crystallization with lawsonite or clinozoisite in the metasediments of the Punta Balandra nappe indicates a further temperature increase to upper blueschist and lawsonite-eclogite facies conditions, as enclosed eclogite facies metabasites.

The P–T paths for the Samaná complex nappes (Fig. 5) can be divided into three general stages related to specific metamorphic events (M1 to M3; Escuder-Viruete et al., 2011).

(1) The pre-D2 segment in the Punta Balandra, Santa Bárbara and Rincón nappes preserved in the S1 fabric relicts in metasediments and mafic eclogites. This P–T segment belongs to the carpholite and lawsonite (±glaucophane) stability fields and defines an M1 prograde path from about 300 to 350 °C and 10–12 kbar to the garnet-free (Santa Bárbara and Rincón) and the garnet-bearing (non-mélange Punta Balandra) lawsonite blueschists facies conditions. In enclosed mafic eclogites, garnet growth with stable lawsonite + omphacite (+Phg + Pg + Chl) indicates low-P lawsonite-eclogite facies conditions. In eclogites of the uppermost mélange, this syn-D1 to early syn-D2 P–T segment records rising P and T to the thermal peak (22–24 kbar at 610–630 °C; Escuder-Viruete and Pérez-Estaún, 2006), which is located in the phengite-bearing eclogitic field (±Pg).

(2) The syn- to late-D2 segment is characterized by M2 decompression and cooling in all nappes (Fig. 5), from the eclogitic peak conditions to epidote-blueschist (8–12 kbar at 400–500 °C) and greenchist facies conditions (4–8 kbar at 400–350 °C) in the Punta Balandra nappe, and from carpholite and lawsonite-blueschist to upper greenchist facies conditions in the Santa Bárbara and Rincón nappes. The derived retrograde P–T path is sub-parallel to the prograde P–T evolution and indicates cooling during the exhumation of the high-P rocks. It should be noted that the descompresive P–T path of the upper structural levels of the Santa Bárbara Schists nappe was accompanied by a slight heating, forming pseudomorphic clinozoisite + white mica after lawsonite at the epidote-blueschist facies conditions.

(3) The syn-D3 and D4 segment of the late retrograde P–T path ($P < 4$–5 kbar) is characterized by M3 cooling at low-P, and is recorded by the greenschist to subgreenschist-facies S3 cleavage and S4 shear fabrics.

These P–T estimates for the Samaná complex compare well with estimates for adjacent units along strike. Peak metamorphic estimates for the eclogitic blocks in the Jagua Clara serpentinite-matrix mélange of the Río San Juan complex (Krebs et al., 2007), plot on a single low-P/high-T metamorphic gradient of about 8 °C/km.

6.3. Tectonic interpretation of D2 deformation

The Samaná complex is mainly made of Upper Mesozoic platform to pelagic metasediments forming a nappe pile. Macro and mesoscopic D2 structures and gradients of D2 ductile shearing are related to the nappe contacts. Deformation/metamorphism relationships indicate that the nappe pile was largely assembled prior to D3/M3 and therefore formed during D1 and D2. The P–T estimates show that the degree of M1 metamorphism within the Samaná complex increases upward from the Playa Colorada nappe toward the Punta Balandra nappe. Therefore, and because D1 was accompanied and followed by an M1 growth of prograde high-P mineral assemblages, it is suggested that initial stacking of the Samaná complex nappes took place during underthrusting and underplating that caused deep burial and maximum metamorphic pressures. An exception to this scheme of emplacement is the Majagual-Los Cacaos nappe (see below).

The kinematic data for D2 deformation in all nappes supply a regionally consistent top-to-the-NE/E sense of shear (Fig. 10). The P–T conditions calculated for D2 mineral assemblages indicate therefore an NE/E-directed tectonic transport during and shortly after high-P metamorphism. For example, the Punta Balandra nappe (including the uppermost ophiolitic mélange) was emplaced during D2 onto the Santa Bárbara Schists nappe. Deformation/metamorphism relationships show that D2 structures formed during decompression indicating considerable exhumation of the Punta Balandra nappe during D2 (Fig. 5). These constraints also demand that the Punta Balandra basal thrust must have moved upward relative to the latest Eocene/Oligocene Earth's surface in the direction of tectonic transport and therefore resulted from horizontal crustal contraction (cf. Wheeler and Butler, 1994). Thrusting of the Punta Balandra nappe onto a cold foreland unit, i.e. the Santa Bárbara and Rincón nappes ensemble caused cooling of the eclogites and blueschists (Fig. 5). Bucher and Bousquet (2007) described a similar case of initial decompression and rapid cooling during nappe stacking in the Western Alps. In this context, the slight heating of the uppermost structural levels of the Santa Barbara nappe (epidote-in isograd) could be also consequence of downward heat transfer during D2 thrusting. Following arguments exposed previously, the D2 structures formed diachronically in the different tectonic nappes from the Early Eocene to the earliest Oligocene, predating the subaereal exhumation and erosion of the Samaná complex in the Middle/Late Miocene.

On the other hand, the metamorphic data for the different nappes (Table 1) showed that the P–T conditions evolve rather continuously in the complex from 10 to 12 kbar-300–350 °C to 18–20 kbar-450 °C, as exemplified by the progressive southward increase of the Si^{4+}-contents in white mica (reflecting the P-dependent phengitic substitution) in carpholite-, lawsonite-, epidote- or garnet-bearing assemblages (reflecting the T increase toward the upper structural levels; Escuder-Viruete et al., 2011). Subordinate, mafic blocks found in the uppermost mélange-like Punta Balandra nappe, yielded higher P–T values (Escuder-Viruete and Pérez-Estaún, 2006).

In general, the shape of the retrograde P–T path is similar in all units and indicate cooling and decompression in the blueschist facies during the D2 ductile deformation. This syn-D2 tectonometamorphic evolution is interpreted occur since the beginning of accretion of each nappe to an accretionary wedge, where the incorporation of every nappe to the overriding plate implies a jump in the basal thust toward the foreland. Therefore, the Samaná complex represent a fossil collisional accretionary wedge, built with metasediments detached from the underlying oceanic to continental crust during subduction. The exhumation mechanisms in the accretionary wedge were probably driven by underthrusting, detachment faulting and erosion, and the continuity of the P–T conditions within the accreted metasedimentary material were in this case roughly preserved.

However, the pressure drop during D2 thrusting requires the removal of 30–40 km of overburden above the Punta Balandra nappe. There is no definite evidence for Eocene to earliest Oligocene normal faulting in the Río San Juan and Puerto Plata complexes, which probably overly the Samaná complex in western Septentrional Cordillera. The contact between the Majagual-Los Cacaos and the Punta Balandra nappes is a good candidate to be a normal fault since it accommodates an important pressure gap, particularly along the dark-layer of cataclasites. However, mapping indicates that the S2 fabrics and the basal thrust of the Majagual-Los Cacaos nappe are cut by WNW-striking strike-slip faults associated with the Septentrional Fault zone, and the vertical displacement related to this cataclastic horizon could not be evaluated.

6.4. D4 crustal extension

The overall geometric relationship between D4 structures which overprinted the SW-dipping S2 foliations and D2 thrust surfaces, the general attitude of S4 ductile-brittle normal shears, the opposed NE- and SW-vergence of associated D4 subhorizontal folding, and the relatively abundance of D4 top-to-the-SW and NE kinematic indicators, indicates that D4 was caused by horizontal crustal extension. This late extension that affects the nappe pile of the Samaná complex was also documented by Gonçalvez et al. (2000).

Crustal extension during D4 is corroborated by the progressive development from ductile to brittle conditions of D4 structures and S4-L4 fabrics in the D4 shear zones and faults. There, the parallelism between mylonitic L4 stretching lineation and the extension direction as often deduced from fault-slip analysis suggests kinematic compatibility during progressive D4 exhumation. The continuous evolution of these D4 structures from ductile to brittle conditions resembles the structural evolution in the footwall of extensional faults in other well-known nappe complexes subjected to late extension, as the Cycladic Massif in Greece (Jolivet et al., 2003) and the Piedmont complex in the Western Alps (Tricart et al., 2004). Likewise, the similar kinematics of ductile-brittle D4 structures and the brittle overprint at the Majagual-Los Cacaos basal thrust implies a kinematic compatibility during progressive exhumation.

6.5. Temperature-time and pressure-time paths

The Fig. 12 shows the T–t and P–t of the different nappes that constitute the Samaná complex. They are constructed integrating the compilation of metamorphic P–T conditions (Table 2; Fig. 5) and the available geochronological data (Fig. 11). This compilation aims at identifying key T–t and P–t points of the structural evolution of Samaná complex rocks during the building of the accretionay wedge, at constraining general subduction and exhumation processes and rates and, to some extent, at establishing the time of plate interactions at the nortern Caribbean subduction zone (Fig. 13).

6.5.1. Subduction rates

Regional considerations of eastward migration of the Caribbean island-arc during the Mesozoic (Maresch and Gerya, 2005; Pindell and Kennan, 2009) suggest low convergence rates at the Río San Juan "subduction zone" of 20–40 mm/yr, with a long-term average of ~22 mm/yr (Krebs et al., 2007). These estimates agree with the present convergence rate of 21 mm/yr for the Caribbean plate with respect to the North America plate (Mann et al., 2002; Manaker

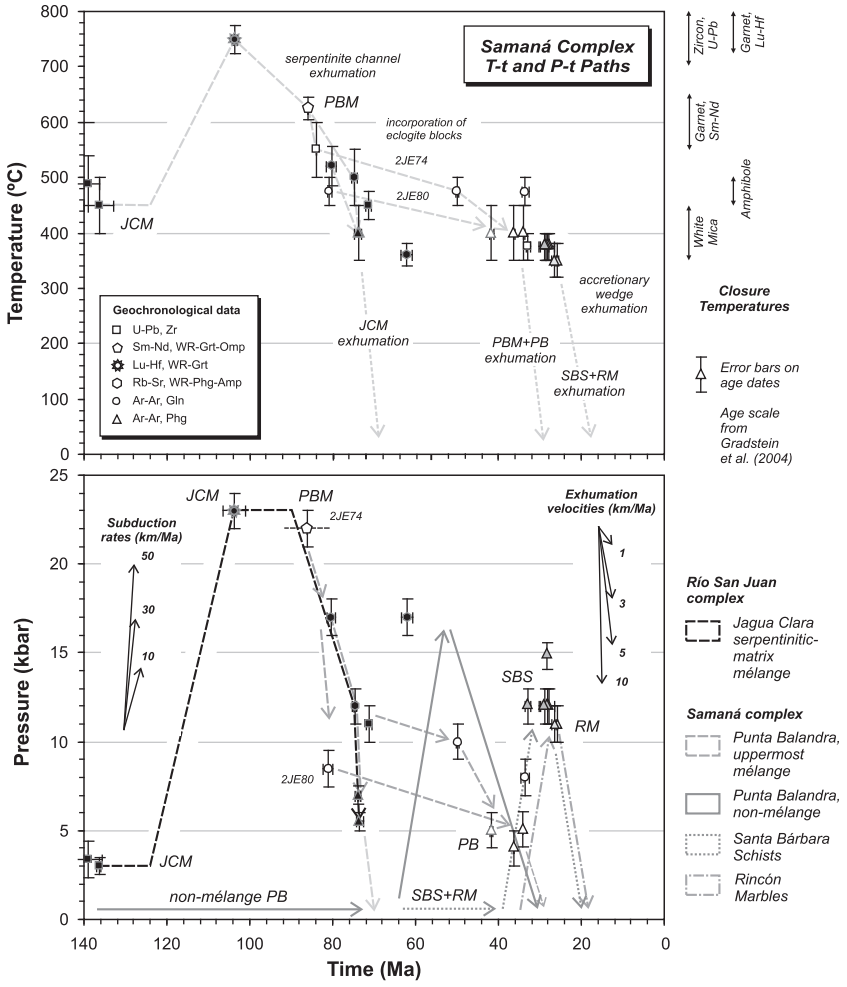

Fig. 12. T–t and P–t paths derived from geochronological and petrological data of the Samaná complex nappes and Jagua Clara mélange of the neighboring Río San Juan complex (Krebs et al., 2007). See text for construction of the model paths and inferred subduction and exhumation rates. JCM = Jagua Clara mélange; RM = Rincón Marbles; SBS = Santa Bárbara Schists; PBM = Punta Balandra mélange; and PB = Punta Balandra non-mélange.

et al., 2008). The term convergence rate is used here to denote the horizontal component of the subduction path. Assuming subduction rates of 30 mm/yr at the pre-collisional northern Caribbean subduction zone and an average geometry of an accretionary wedge (basal décollement ~7°, Davis et al., 1983), and that these subduction rates are largely representative for the Cenozoic, we would expect that subduction to a depth of 56 and 36 km, as deduced from P–T data on Santa Bárbara Schists and Rincón Marbles, would have occurred in about 15.3 and 9.8 Ma, respectively. The latter data suggest that the high-P rocks of Santa Bárbara Schists and Rincón Marbles started to subduct at about 46 (Early Eocene) and 36 Ma (Late Eocene), respectively (Fig. 12). Selecting a higher subduction rate of 50 mm/yr causes the start of subduction at about 44.5 (Middle Eocene) and 32.5 Ma (Eocene-Oligocene boundary), respectively for these two nappes. The resulting burial rates are of 3.6 mm/yr.

The estimate of subduction onset for the Punta Balandra nappe prove to be more uncertain because the age of the pressure peak at about 18–20 kbar in the eclogitic metasediments is not known. Considering the $^{40}Ar/^{39}Ar$ cooling phengite age of 41.7 ± 0.4 Ma in metasediments (at 5 kbar, 4JE125 sample, this work), it is obtained following similar reasonings an age for the subduction to a depth of 60 km (18 kbar, baric peak) of about 52.6 Ma (lowermost Eocene) and the for the start of subduction of sedimentary protoliths of 65.3 Ma (Maastrichtian-Paleocene boundary; after 12.7 Ma de subducción). For a higher subduction rate of 50 mm/yr, ages of 49.6 Ma for the eclogitic peak (Early Eocene) and of 59.9 Ma for the start of subduction (Paleocene; after 10.5 Ma of subduction) are obtained.

These relations suggest that in the meantime the Punta Balandra nappe exhumes the Santa Bárbara Schists and slightly older the Rincón Marble nappes are buried, which reinforces the structural interpretation of thrusting of the first unit onto the second one during the D2 ductile deformation. From the shape of the retrograde P–T path and the range of $^{40}Ar/^{39}Ar$ phengite cooling ages between 38 and 33 Ma for the Punta Balandra nappe, it is possible to date the beginning of accretion of the Santa Bárbara nappe to the overriding collisional accretionary wedge at the Late Eocene (Fig. 12).

6.5.2. Onset of continental collision at Hispaniola

Fig. 12 also includes the T–t and P–t paths derived from petrological and geochronological data for eclogite blocks of the Jagua Clara serpentinitic-matrix mélange of the Río San Juan complex obtained for Krebs et al. (2007). These authors estimated minimum ages of ~124 Ma for the initiation of subduction bellow the Caribbean island-arc, and ages of ~74–62 Ma for cooling below 400 °C during exhumation of the eclogite and blueschist blocks. Therefore, onset of the high-P metamorphism in the Samaná complex nappes occurred afterward (except some mafic eclogite blocks, see below). However, the latest ages of

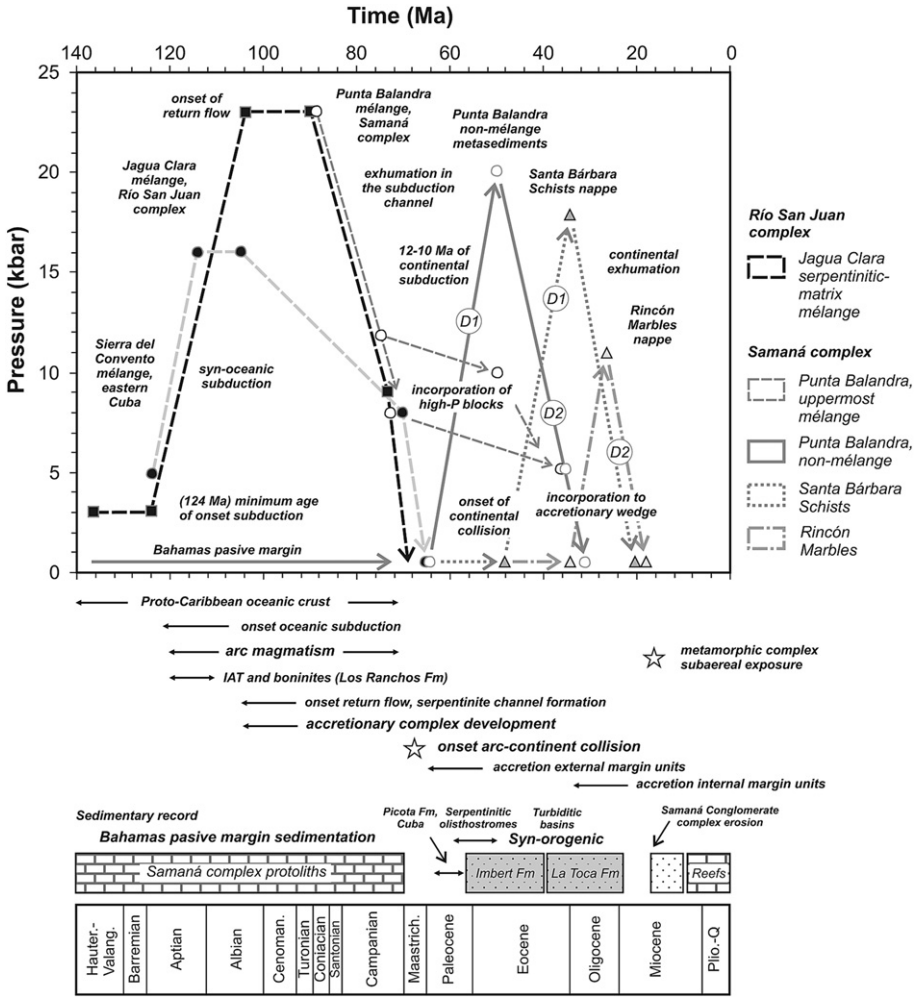

Fig. 13. Model multistage and diachronic P–t paths for the Jagua Clara mélange and Samaná complex nappes including the syn-oceanic subduction, onset of return flow in the subduction channel, cooling in the upper plate, syn-oceanic exhumation for oceanic rocks, onset of arc-continent collision, continental margin subduction, and continental exhumation stages. See text for construction of the model paths, particularly for the exotic mafic eclogite blocks enclosed in the Punta Balandra mélange. Schematic P–t path of the Sierra del convento mélange in eastern Cuba (Lázaro et al., 2008) is shown for reference. Also, the time interval for Caribbean island-arc magmatism, high-P accretionary complex development, onset of arc-continental collision, and the record of Bahamas passive margin sedimentation, syn-orogenic sedimentation and final subaereal exposure of the Samaná metamorphic complex are also included.

exhumation in high-P blocks of the Jagua Clara mélange (Krebs et al., 2007), our crude estimate for the onset of subduction of the non-mélange Punta Balandra nappe metasediments, which probably belong to the more distal Bahamas margin, and the Paleocene?-Lower Eocene age of the syn-orogenic serpentinitic olistostromes of the lower Imbert Fm (Draper and Nagle, 1991), which indicates the surface exposure of the serpentinitic-matrix mélange (Escuder-Viruete, 2009a), cluster in a relatively narrow time interval (60 ± 5 Ma; Fig. 13). It is suggested that this time marks the obstruction of subduction zone in the Hispaniola segment of the northern Caribbean convergent margin, the onset of accretion of the more distal Bahamas margin to the Caribbean plate, and the subsequent propagation of the deformation front toward the northeast (i.e. the foreland). This age is also consistent with the end of sedimentation in the passive Bahamian continental margin (Iturralde-Vinent et al., 2006), the Campanian-Maastrichtian age of the youngest meta-carbonates incorporated in the accretionary wedge at Samaná complex (Weaver et al., 1976), and of the cessation of volcanism in the Caribbean island-arc (Fig. 13; Escuder-Viruete et al., 2009).

Note that a similar P–T path has recently been deduced by Lázaro et al. (2008) for contemporaneous subducted blocks of amphibolites and related trondhjemites in the Sierra del Convento serpentinitic-matrix mélange, eastern Cuba, probably formed in the same subduction environment as the Río San Juan complex. For this reason, the general P-t path for the subducted blocks is also included in the Fig. 13. These authors describe a syn-collisional stage of exhumation of the mélange between 70 and 65 Ma, with a surface exposure constrained by the age of the syn-orogenic olistostromal La Picota Fm (68–63 Ma: García-Casco et al., 2009), contemporaneous with the initial exhumation of mafic eclogites in the Río San Juan and the mélange part of Punta Balandra nappe.

6.5.3. *Mafic eclogite blocks in the mélange-like Punta Balandra nappe*

Although the studied blocks of mafic eclogites in the mélange part of the Punta Balandra nappe present a similar and coeval retrograde metamorphic evolution in the Eocene, several arguments suggest a post-peak tectonic interleaving of eclogites and enclosing high-P metasediments. These include: (1) peak conditions at different times (Late Cretaceous *versus* Eocene) and distinctly lower P–T conditions (22–24 kbar at 610–630 °C *versus* 16–20 kbar at 450–500 °C; Escuder-Viruete et al., 2011); (2) mafic

eclogites have a IAT to N-MORB/BABB geochemistry and a weak to moderate subduction-related signature, and the protoliths are interpreted to form in an island-arc to mid-oceanic rift settings (Perfit et al., 1982; Joyce, 1991; Sorensen et al., 1997; Escuder-Viruete et al., 2009); (3) the low Nb contents and the $(La/Yb)_N<4$ values of eclogites, as well as the high $(\epsilon_{Nd})_i = +7.2$ value obtained for 2JE74 eclogite, are most typical of primitive Caribbean island-arc tholeiitic and boninitic magmas (Escuder-Viruete, 2008b); the structural association with other blocks of (ophiolitic) serpentinized peridotites and serpentinitic schists in the mélange part of the Punta Balandra nappe; and (5) the eclogite blocks often have an external rind composed by Mg-rich chlorite, tremolite and fuchsite, probably formed in an older stage of metasomatic interaction between the block and an ultramafic serpentinitic-matrix (Giaramita and Sorensen, 1994). On the other hand, some eclogite and Omp-bearing blueschist blocks of the Rio San Juan complex have a similar age for the pressure peak (~103–80Ma; Fig. 12), comparable IAT and N-MORB whole rock geochemical signature (Escuder-Viruete, 2009a), and are enclosed in the serpentinitic-matrix mélange of Jagua Clara, which has been interpreted by Krebs et al. (2007) as a subduction channel.

All these relations indicate that the studied eclogites are exotic blocks coming from a subduction channel, like the Jagua Clara mélange, which were incorporated to the highermost structural levels of the Punta Balandra nappe during its accretion in eclogite to blueschist facies conditions, i.e. during continental collision. Also, this argument suggests from a structural point of view that the Jagua Clara mélange of the Rio San Juan complex regionally overlies the Samaná complex and crop out in a more internal position in the collisional belt.

Kinematic indicators for the early orogenic evolution in the Caribbean are scarce. In the Septentrional Cordillera, the only shear sense data for deformation associated with blueschist facies metamorphism are those described by Escuder-Viruete (2009a) from the Jagua Clara serpentinitic-matrix mélange of the Río San Juan complex, which also indicate a general top-to-the-ENE tectonic transport. These shear sense indicators are asymmetric strain shadows of glaucophane around garnet in retrograded rims of mafic eclogite blocks, and folded tonalite-trondhjemite pods in antigorite-bearing serpentinitic schist. However, these structures are Campanian to Maastrichtian in age (Krebs et al., 2007; Escuder-Viruete et al., 2009). Late Cretaceous top-to-the-ENE tectonic transport toward the foreland is in accord with Eocene to earliest Oligocene top-to-the-ENE tectonic transport in the nappes of an underlying Samaná complex, the Late Oligocene high-P metamorphism in the most external Rincón Marbles nappe, and a general northeastward progradation of deformation in the northern Caribbean.

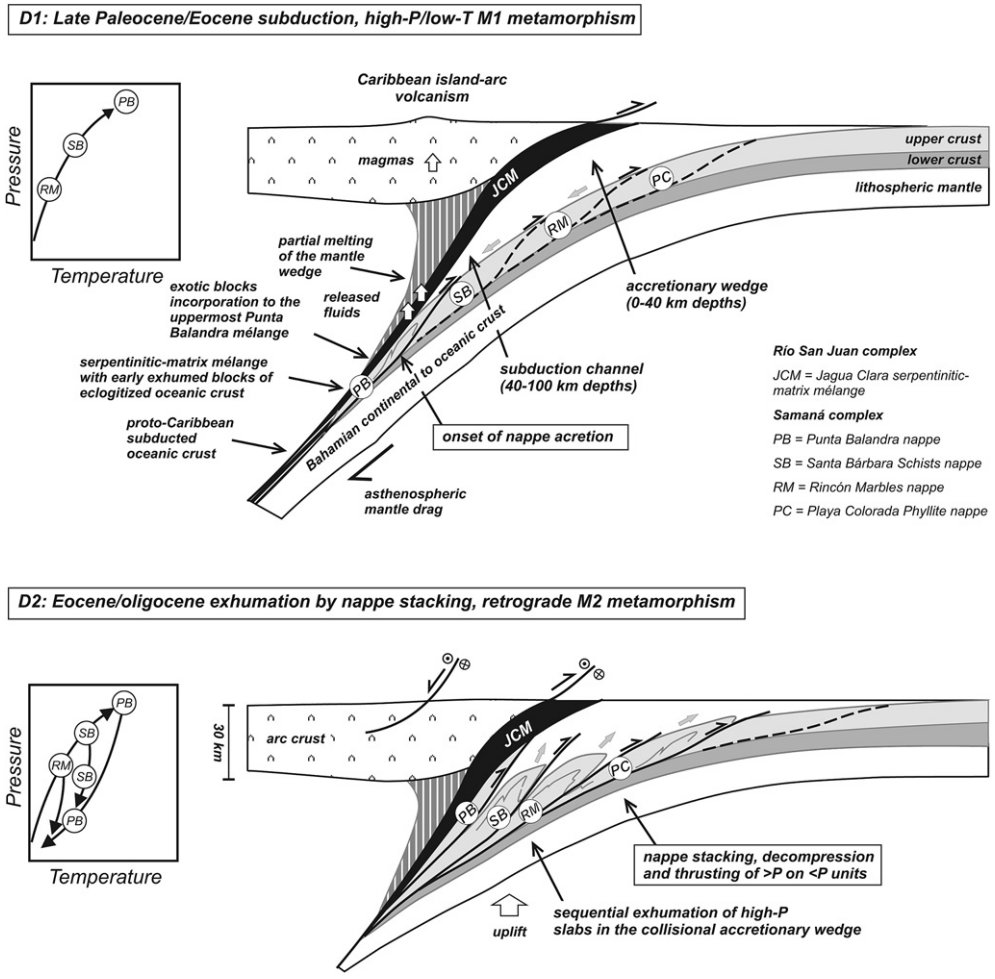

Fig. 14. Schematic model for the structural and metamorphic evolution of the Samaná complex based on the interpretation of the isotopic data, showing the key processes controlling the exhumation of high-P rocks in an accretionary wedge formed during arc-collision. Two main stages can be distinguished: D1, prograde high-P metamorphism just the onset of nappe accretion to the orogenic wedge; and D2, nappe stacking, decompression, retrograde metamorphism, and thrusting of higher-P onto lower-P structural nappes.

6.5.4. Exhumation rates

Assuming the closure temperatures discussed above, the P–T data summarized in Table 1 and the geochronological results included in Fig. 11 can be used to calculate exhumation rates (Fig. 12). Considering the subaereal exposure of the Samaná complex at ~14 Ma (as clasts in the Middle Miocene Samaná Conglomerate), exhumation rates from the maximum attained depth are of 2.6 mm/yr for the Santa Bárbara Schists and of 2.9 mm/yr for the Rincón Marbles. These exhumation rates are similar to those obtained in other metasedimentary accretionary wedges, as the Schistes Lustrés of the Western Alps and the Cascadian, Franciscan and Chilean examples (~2–3 mm/yr see compilation of Agard et al., 2009). In the P–t path of exhumation of the mafic eclogite blocks in the Jagua Clara mélange two segments characterized by a different exhumation rate are observed (Figs. 12 and 13): a first segment from the eclogitic peak at 103 Ma to the epidote-blueschist stage at 75–73 Ma with exhumation rates of 1.4 mm/yr; and a second segment to the final surface exposition of the rocks at 65–60 Ma (as breccias and clasts in the serpentinitic olisthostromes of the lower Imbert Fm) with exhumation rates between 7.6 and 3.6 mm/yr. Different velocities can be explained by exhumation in two contrasted settings: a first stage of slow exhumation in the subduction channel, largely lower to plate velocities; and a second stage of fast exhumation up to surface. Therefore, the exhumation was temporarily discontinuous and the velocity increase probably triggered in reponse to the entrance of bouyant material in the subduction wedge, as the crust of a thinned continental margin (Yamato et al., 2007; Agard et al., 2009).

7. Conclusions

The new structural and geochronological data presented in this study further constrain the timing of the intra-oceanic subduction and continental collision in the northern Caribbean convergen margin preserved within the Septentrional Cordillera of Hispaniola domain as summarized in Fig. 14. In the following we integrate the isotopic ages into a tectonothermal model and make an attempt to construct a complete P-T-D-t path for the high-P metasedimentary nappes of the Samaná complex.

Sediment-accretion and subduction (60–35 Ma; D1). The nappe pile of the Samaná complex is interpreted to have formed an accretionary wedge during Cenozoic subduction of the proto-Caribbean ocean, followed by the subduction of the more distal North America margin beneath the Caribbean upper plate (and previously accreted micro-continents). The age of the youngest metasediments within this collisional accretionary wedge is Campanian-Maastrichtian (Weaver et al., 1976). The high-P/low-T M1 metamorphic mineral assemblages and relics in syn-metamorphic quartz-calcite veins formed during the first deformation event D1. $^{40}Ar/^{39}Ar$ plateau ages on phengite, T–t/P-t estimations and regional isotopic age data revealed Eocene to Late Oligocene high-P metamorphism in the different nappes, conform they are sequentially incorporated to the accretionary wedge.

Nappe stacking and exhumation (35–25 Ma; D2). Nappe stacking in the Samaná complex was associated with substantial exhumation of the blueschist facies rocks (Fig. 5). The retrograde mineral assemblages (Table 2) and thermobarometric calculations (Escuder-Viruete et al., 2011) indicate decompression under nearly isothermal or cooling conditions. All $^{40}Ar/^{39}Ar$ plateau ages in this 35–25 Ma time interval were obtained on phengite and interpreted to record cooling or growth at their closure temperature during decompression that is contemporaneous with D2 nappe stacking. T–t and P–t estimations revealed Late Eocene to earliest Miocene retrograde M2 metamorphism in the different nappes, top-to-the-ENE tectonic transport towards the foreland and a general northeastward progradation of deformation in the northern Caribbean.

Late deformations (D3, D4 and D5). The D3 nappe re-folding event substantially modified the nappe stack in the Samaná complex and produced open to tight folds with amplitudes up to kilometer-scale. The D4 ductile to brittle normal shear zones and faults record a late extensional deformation, which also affects the whole nappe pile of the Samaná complex. Non-penetrative D3 and D4 fabrics indicate M3 cooling in the greenschist-facies conditions. These late deformations are probably associated with ongoing accretion of thicker continental basement and unroofing. Subsequently, from the Lower Miocene to the Present (Mann et al., 2002), the nappe pile was cut and laterally displaced by a D5 regional system of sinistral strike-slip and reverse faults associated with the Septentrional fault zone.

Acknowledgments

Constructive criticism and comments by the two reviewers Gren Draper and Antonio García-Casco and editorial handling by Robert Holdsworth are acknowledged. The Dirección General de Minería of the Dominican Government is also thanked by assistance. Funding by the Spanish Ministerio Ciencia e Innovación project CGL2009-08674/BTE and precursor project CGL2005-02162/BTE is gratefully acknowledged. This work also received aid from the cartographic project of the Dominican Republic funded by the SYSMIN Program of the European Union and is a contribution to IGCP-546 "Subduction zones of the Caribbean" and Topo-Iberia Consolider-Ingenio (2010 CSD2006-00041).

Appendix. Supplementary data

Supplementary data associated with this article can be found in online version, at doi:10.1016/j.jsg.2011.02.006.

References

Agard, P., Jolivet, L., Goffé, B., 2001. Tectonometamorphic evolution of the Schistes Lustrés complex: implications for the exhumation of HP and UHP rocks in the Western Alps. Bulletin Societe Geologique France 172 (5), 617–636.

Agard, P., Yamato, P., Jolivet, L., Burov, E., 2009. Exhumation of oceanic blueschists and eclogites in subduction zones: timing and mechanisms. Earth-Science Reviews 92, 53–79.

Bousquet, R., Oberhänsli, R., Goffé, B., Jolivet, L., Vidal, O., 1998. High-pressure-low temperature metamorphism and deformation in the Bündnerschiefer of the Engadine window: implications for the regional evolution of the eastern Central Alps. Journal of Metamorphic Geology 16, 657–674.

Bousquet, R., Goffé, B., Vidal, O., Patriat, M., Oberhänsli, R., 2002. The tectonometamorphic history of the Valaisan domain from theWestern to the Central Alps: new constraints for the evolution of the Alps. Geological Society American Bulletin 114, 207–225.

Bucher, K., Frey, M., 2002. Petrogenesis of Metamorphic Rocks, seventh ed. Springer, Berlin, 341 pp.

Bucher, S., Bousquet, R., 2007. Metamorphic evolution of the Briançonnais units along the ECORSCROP profile (Western Alps): new data on metasedimentary rocks. Swiss Journal of Geosciences 100, 227–242.

Catlos, E.J., Sorensen, S.S., 2003. Phengite-based chronology of K- and Na-rich fluid flow in two paleosubduction zones. Science 299, 92–95.

Cloos, M., Shreve, R.L., 1988. Subduction-channel model of prism accretion, melange formation, sediment subduction, and subduction erosion at convergent plate margins: 1. Background and description. Pure Applied Geophysics 128, 455–499.

Chopin, C., 2003. Ultrahigh-pressure metamorphism: tracing continental crust into the mantle. Earth and Planet Science Letters 212, 1–14.

Davis, D., Suppe, J., Dahlen, F.A., 1983. Mechanics of fold-and- thrust belts and accretionary wedges. Journal of Geophysical Research 88, 1153–1172.

De Zoeten, R., Draper, G., Mann, P., 1991. Geological map of the northern Dominican republic. In: Mann, P., Draper, G., Lewis, J.F. (Eds.), Geologic and Tectonic Development of the North America-Caribbean Plate Boundary in Española. Geological Society of America Special Paper, 262 Plate 1.

Draper, G., Lewis, J.F., 1991. Geologic map of the Central Dominican republic (1:150,000). In: Mann, P., Draper, G., Lewis, J.F. (Eds.), Geological and Tectonic

Development of the North American-Caribbean Plate Boundary in Hispaniola. Geological Society America Special Paper, 262 (plates).
Draper, G., Nagle, F., 1991. Geology, structure and tectonic develoopment of the Río San Juan complex, northern Dominican republic. In: Mann, P., Draper, G., Lewis, J. (Eds.), Geologic and Tectonic Development of the North America-Caribbean Plate Boundary Zone in Hispaniola. Geological Society America Special Paper, 262, pp. 77–95.
Draper, G., Mann, P., Lewis, J.F., 1994. Hispaniola. In: Donovan, S.K., Jackson, T.A. (Eds.), Caribbean Geology: An Introduction. University of the West Indies Publishers Association, Kingston, Jamaica, pp. 129–150.
Ernst, W.G., 2005. Alpine and Pacifi c styles of Phanerozic mountain building: subduction-zone petrogenesis of continental crust. Terra Nova 17, 165–188.
Escuder-Viruete, J., 2008a. Mapa Geológico de la República Dominicana E. 1:50.000, Santa Bárbara de Samaná (6373-IV). Dirección General de Minería, Santo Domingo, 197 pp.
Escuder-Viruete, J., 2008b. Petrología y Geoquímica de Rocas Ígneas y Metamórficas: Hojas de Las Galeras, Santa Bárbara de Samaná y Sánchez. Informe Complementario al Mapa Geológico de la República Dominicana a E. 1:50.000. IGME-BRGM, Santo Domingo, 79 pp.
Escuder-Viruete, J., 2009a. Mapa Geológico de la República Dominicana E. 1:50.000, Río San Juan (6174-I). Dirección General de Minería, Santo Domingo, 223 pp.
Escuder-Viruete, J., Pérez-Estaún, A., 2004. Trayectoria metamórfica P-T relacionada con subducción en eclogitas del Complejo de Basamento de Samaná, Cordillera Septentrional, República Dominicana. Geo-Temas 6, 37–44.
Escuder-Viruete, J., Pérez-Estaún, A., 2006. Subduction-related P-T path for eclogites and garnet glaucophanites from the Samaná Peninsula basement complex, northern Hispaniola. International Journal of Earth Sciences 95, 995–1017.
Escuder-Viruete, J., Friedman, R., Pérez-Estaún, A., Joubert, M., Weis, D., 2009. U-Pb constraints on the timing of igneous and metamorphic events in the Rio San Juan complex, northern Hispaniola VII Congreso Cubano de Geología. Workshop IGCP-544.
Escuder-Viruete, J., Pérez-Estaún, A., Booth-Rea, G., Valverde-Vaquero, P., 2011. Tectonometamorphic evolution of the Samaná complex, northern Hispaniola: implications for the burial and exhumation of high-pressure rocks in a collisional accretionary wedge. Lithos. doi:10.1016/j.lithos.2011.02.006.
García-Casco, A., Torres-Roldán, R.L., Iturralde-Vinent, M.A., Millán, G., Núñez Cambra, K., Lázaro, C., Rodríguez Vega, A., 2006. High pressure metamorphism of ophiolites in Cuba. Geologica Acta 4, 63–88.
García-Casco, A., Iturralde-Vinent, M.A., Pindell, J., 2009. Latest Cretaceous collision/accretion between the Caribbean plate and Caribeana: Origin of metamorphic terranes in the Greater Antilles. International Geological Review.
Gerya, T.V., Stoeckhert, B., Perchuk, A.L., 2002. Exhumation of high-pressure metamorphic rocks in a subduction channel — a numerical simulation. Tectonics 21 6–1 – 6–19.
Giaramita, M.J., Sorensen, S.S., 1994. Primary fluids in lowtemperature eclogites - Evidence from 2 subduction complexes (Dominican Republic, and California, USA). Contributions Mineralogy and Petrology 117, 279–292.
Goffé, B., Bousquet, R., 1997. Ferrocarpholite, chloritoïde et lawsonite dans les métapelites des unités du Versoyen et du Petit St Bernard (zone valaisanne, Alpes occidentales). Schweizerische Mineralogische und Petrographische Mitteilungen 77, 137–147.
Gonçalves, Ph., Guillot, S., Lardeaux, J.M., Nicollet, C., Mercier de Lépinay, B., 2000. Thrusting and sinistral wrenching in a pre-Eocene HP-LT Caribbean accretionary wedge (Samaná peninsula, Dominican republic). Geodinamica Acta 13, 119–132.
Guillot, S., Hattori, K.H., de Sigoyer, J., Nägler, T., Auzende, A.L., 2001. Evidence of hydration of the mantle wedge and its role in the exhumation of eclogites. Earth and Planetary Science Letters 193, 115–127.
Guillot, S., Schwartz, S., Hattori, K., Auzende, A., Lardeaux, J., 2004. The Monviso ophiolitic Massif (Western Alps), a section through a serpentinite subduction channel. In: Beltrando, M., Lister, G., Ganne, J., Boullier, A. (Eds.), Evolution of the Western Alps: Insights from Metamorphism, Structural Geology, Tectonics and Geochronology, The Virtual Explorer. pp. Paper 3.
Guillot, S., Hattori, K., Agard, P., Schwartz, S., Vidal, O., 2009. Exhumation processes in oceanic and continental subduction contexts: a review. In: Lallemand, S., Funiciello, F. (Eds.), Subduction Zone Geodynamics. Springer-Verlag Berlin Heidelberg 175-205 p. DOI: 10.1007/978-3-540-87974-9.
Heard, H.C., Raleigh, C.B., 1972. Steady state flow in marble at 500 °C to 800 °C. Geological Society of America Bulletin 83, 935–956.
Hermann, J., Müntener, O., Scambelluri, M., 2000. The importance of serpentinite mylonites for subduction and exhumation of oceanic crust. Tectonophysics 327, 225–238.
Iturralde-Vinent, M.A., Díaz Otero, C., Rodríguez Vega, A., Díaz Martínez, R., 2006. Tectonic implications of paleontologic dating of Cretaceous-Danian sections of Eastern Cuba. Geologica Acta 4, 89–102.
Jolivet, L., Faccenna, C., Goffé, B., Burov, E., Agard, P., 2003. Subduction tectonics and exhumation of high-pressure metamorphic rocks in the Mediterranean orogens. American Journal of Science 303, 353–409.
Joyce, J., 1991. Blueschist metamorphism and deformation on the Samaná peninsula: a record of subduction and collision in the Greater Antilles. In: Mann, P., Draper, G., Lewis, J. (Eds.), Tectonic development of the north America-Caribbean plate boundary zone in Hispaniola. Geological Society America Special Paper, 262, pp. 47–75.
Joyce, J., Aronson, J., 1987. K-Ar Ages for Blueschist Metamorphism on the Samaná Peninsula. Dominican Republic. Transac 10th Caribbean Geolog Conference, Cartagena, Colombia, pp. 454–458.
Kimura, G., Maruyama, S., Isozaki, Y., Terabayashi, M., 1996. Well-preserved underplating structure of the jadeitized Franciscan compex, Pacheco Pass, California. Geology 24, 75–78.
Krebs, M., Maresch, W.V., Schertl, H.-P., Baumann, A., Draper, G., Idleman, B., Münker, C., Trapp, E., 2007. The dynamics of intra-oceanic subduction zones: a direct comparison between fossil petrological evidence (Rio San Juan Complex, Dominican Republic) and numerical simulation. Lithos 103, 106–137. doi:10.1016/j.lithos.2007.09.003.
Lázaro, C., García-Casco, A., Rojas Agramonte, Y., Kröner, A., Neubauer, F., Iturralde-Vinent, M.A., 2008. Fifty-five-million-year history of oceanic subduction and exhumation at the northern edge of the Caribbean plate (Sierra del Convento Mélange, Cuba). Journal of Metamorphic Geology 27, 19–40.
Lister, G.S., Forster, M., 1996. Inside the Aegean Metamorphic Core Complexes. Technical Publication Australian Crustal Research Centre. 45, 110 p.
Manaker, D.M., Calais, E., Freed, A.M., Ali, S.T., Przybylski, P., Mattioli, G., Jansma, P., Prépetit, C., de Chabalier, J.B., 2008. Interseismic Plate coupling and strain partitioning in the Northeastern Caribbean. Geophysical Journal International 174, 889–903. doi:10.1111/j.1365-246X.2008.03819.x.
Mann, P., 1999. Caribbean sedimentary basins: classification and tectonic setting from Jurassic to present. In: Mann, P. (Ed.), Caribbean Basins. Sedimentary Basins of the Word, 4, pp. 3–31.
Mann, P., 2007. Global catalogue, classification and tectonic origins of restraining- and releasing bends on active and ancient strike-slip fault systems. In: Cunningham, W.D., Mann, P. (Eds.), Tectonics of Strike-Slip Restraining and Releasing Bends. Geological Society London Special Publications, 290, pp. 13–142.
Mann, P., Calais, E., Ruegg, J.C., DeMets, C., Jansma, P.E., Mattioli, G.S., 2002. Oblique collision in the northeastern Caribbean from GPS measurements and geological observations. Tectonics 21, 1057–1082.
Maresch, W.V., Gerya, T.V., 2005. Blueschists and blue amphiboles: how much subduction do they need? International Geological Review 47, 688–702.
McDougall, I., Harrison, T.M., 1999. Geochronology and Thermochronology by the $^{40}Ar/^{39}Ar$ Method. Oxford Universitiy Press, New York and Oxford. 269 p.
Perfit, M.R., Nagle, F., Bowin, C.O., 1982. Petrology and Geochemistry of Eclogites and Blueschists from Hispaniola. 1st International Eclogite Conference, Clermont-Ferrand, France, p. 20.
Pindell, J., Kennan, L., 2009. Tectonic evolution of the Gulf of Mexico, Caribbean and northern South America in the mantle reference frame: an update. In: James, K., Lorente, M.A., Pindell, J. (Eds.), The Geology and Evolution of Region between North and South America. Geological Society of London, Special Publication, 328, pp. 1–55.
Platt, J.P., 1993. Exhumation of high-pressure rocks: a review of concepts and processes. Terra Nova 5, 119–133.
Rimmelé, G., Oberhänsli, R., Goffé, B., Jolivet, L., Candan, O., Cetinkaplan, M., 2003. First evidence of high-pressure metamorphism in the "Cover Series" of the southern Menderes Massif. Tectonic and metamorphic implications for the evolution of SW Turkey. Lithos 71, 19–46.
Rimmelé, G., Parra, T., Goffe, B., Oberhänsli, R., Jolivet, L., Candan, O., 2005. Exhumation paths of high-pressure-low-temperature metamorphic rocks from the Lycian Nappes and the Menderes Massif (SW Turkey): a multi-equilibrium approach. Journal of Petrology 46, 641–669.
Ring, U., Brandon, M.T., 1994. Kinematic data for the Coast Range fault and implications for exhumation of the Franciscan subduction complex. Geology 22, 735–738.
Ring, U., Laws, S., Bernet, M., 1999. Structural analysis of a complex nappe sequence and late-orogenic basins from the Aegean Island of Samos, Greece. Journal of Structural Geology 21, 1575–1601.
Ring, U., Layer, P.W., 2003. High-pressure metamorphism in the Aegean, eastern Mediterranean: underplating and exhumation from the Late Cretaceous until the Miocene to Recent above the retreating Hellenic subduction zone. Tectonics 2, 1022.
Schwartz, S., Lardeaux, J.M., Guillot, S., Tricart, P., 2000. Diversité du métamorphisme éclogitique dans le massif ophiolitique du Monviso (Alpes occidentales, Italie). Geodinamica Acta 13, 169–188.
Sorensen, S.S., Grossman, J.N., Perfit, M.R., 1997. Phengite-hosted LILE enrichment in eclogite and related rocks: implications for fluid-mediated mass transfer in subduction zones and arc magma genesis. Journal of Petrology 38, 3–34.
Spear, F.S., 1993. Metamorphic Phase Equilibria and Pressure-Temperature-Time Paths. Mineral Society of America Monograph Washington, DC.
Stanek, K.P., Maresch, W.V., Grafe, F., Grevel, C., Baumann, A., 2006. Structure, tectonics and metamorphic development of the Sancti Spiritus Dome (eastern Escambray massif, Central Cuba). Geologica Acta 4, 151–170.
Stern, R.J., 2004. Subduction initiation: spontaneous and induced. Earth and Planetary Science Letters 226, 275–292.
Tricart, P., Schwartz, S., Sue, C., Lardeaux, J.M., 2004. Evidence for synextensional tilting and doming during during fi nal exhumation from analysis multistage faults (Queyras, Schsites Lustrés, Western Alps). Journal Structural Geology 26, 1633–1645.
Tsujimori, T., Matsumoto, K., Wakabayashi, J., Liou, J.G., 2006. Franciscan eclogite revisited: reeavaluation of the P–T evolution of tectonic blocks from Tiburon Peninsula, California. USA. Mineralogy and Petrology 88, 243–267.

Vidal, O., Goffé, B., Theye, T., 1992. Experimental study of the stability of sudoite and magnesiocarpholite and calculation of a new petrogenetic grid for the system FeO-MgO-Al_2O_3-SiO_2-H_2O. Journal of Metamorphic Geology 10, 603–614.

Wakabayashi, J., 1990. Counterclockwise P–T–t paths from amphibolites, Franciscan complex, California: relics from the early stages of subduction zone metamorphism. Journal of Geology 98, 657–680.

Weaver, J.D., Panella, G., Llinas-Castellan, 1976. Preliminary sketch of the tectonic history of the Samaná Peninsula, Dominican Republic, presented at 3rd Congresso Latino-Americano de Geologia (Mexico).

Wheeler, J., Butler, R.W.H., 1994. Criteria for identifying structures related to true crustal extension in orogens. Journal of Structural Geology 16, 1023–1027.

Yamato, P., Agard, P., Burov, E., Le Pourhiet, L., Jolivet, L., Tiberi, C., 2007. Burial and exhumation in a subduction wedge: mutual constraints from thermomechanical modeling and natural P-T-t data (Sch. Lustrés, W. Alps). Journal of Geophysical Research 112, B07410. doi:10.1029/2006JB004441.

Zack, T., Rivers, T., Brumm, R., Kronz, A., 2004. Cold subduction of oceanic crust: implications from a lawsonite eclogite from the Dominican Republic. European Journal Mineralogy 16, 909–916.